CHARACTERIZATION OF ELECTROCHEMICALLY SYNTHESIZED PANI/GOD/MWNTs COMPOSITE

A Thesis Submitted

In Partial fulfilment of the requirements for the degree of

MASTER OF TECHNOLOGY

IN

MATERIALS SCIENCE AND ENGINEERING

By

INDU BAJPAI

ROLL No.:60702004

SCHOOL OF PHYSICS AND MATERIAL SCIENCE

THAPAR UNIVERSITY

PATIALA-147004, INDIA

July, 2009

Dedicated to my

Parents

CERTIFICATE

This is to certify that the thesis entitled **"Characterization of Electrocnemically synthesized PANI/GOD/MWNTs composite"** submitted by **Ms. INDU BAJPAI** Roll No. 60702004 in partial fulfillment of the requirement for the award of the degree of **MASTER OF TECHNOLOGY** in Materials Science and Engineering, Thapar University Patiala, is a record of candidate's own work carried out by her under our supervision. The matter embodied in this report is of the candidate's own record and not submitted to any other university in any part or full form for the award of such kind of a degree.

The thesis work has been carried out from 05-01-2009 to 15-07- 2009.

Supervisors

Dr. Lalit M. Bharadwaj
Associate Director& Head
BEND
CSIO
Chandigarh

Dr. Amit L. Sharma
Scientist- C
BEND
CSIO
Chandigarh

Dr. Dwijendra Pratap Singh
Lecturer
School of Physics and
Materials Science,
Thapar University, Patiala

Countersigned by:

(Dr. O.P. Pandey)
Professor& Head
Thapar University
Patiala

(Dr. R.K. Sharma)
Dean, Academic Affairs
Thapar University
Patiala

Dated: 14 July 2009

ACKNOWLEDGEMENT

I would like to express my deepest gratitude to my supervisor Dr. Lalit M. Bharadwaj for the inspiring guidance, support, encouragement and time commitment during this thesis. I would like to thanks to Dr. Amit L. Sharma for his help and support. I could not finish my study without their help and encouragement. I believe what I have learnt from them would greatly benefit my future career. I would also like to acknowledge the contribution of my supervisor Dr. Dwijendra Pratap Singh.

I wish to express my sincere thanks to Dr. Pawan Kapoor (Director CSIO), and Dr. O.P. Panday, Professor and head, School of Physics and Materials Science for permitting and providing the facilities necessary for carrying out thesis work at CSIO.

I am thankful to Dr. Akash Deep, Dr. Indrapreet Kaur, Mr. Ashwani Kumar, Ms. Harsimran Kaur, Mr. Suresh Kumar, Mr. Deepak Kukkar of Biomolecular Electronics and Nanotechnology Division, CSIO, for their much appreciated guidance.

I would also like to give many thanks and best wishes to my fellow trainees in BEND, CSIO, for any kind of help and valuable suggestions.

I am highly grateful to Professor K. K. Raina, and Dr. Kulvir Singh, School of Physics And Material Science, Thapar University Patiala (Punjab) for their kind help and valuable suggestions and special attention throughout my work. It is due to their moral encouragement, love and providing me fountain of inspiration all shorts of assistance from time to time into up-bringing me up to this stage.

I would also like to give many thanks my friends Mr. Sandeep Kumar Singh, Mr. Karuna Sagar Chaturvedi, Mr. Arun Kumar, Mr. Neetesh Kumar, Ms. Supriya Saxena, Mr. Ravi Shukla and my colleagues at the School of Physics and Material Sciences are acknowledged for providing me a friendly atmosphere and encouraging me throughout this work.

I am deeply thankful to my Family, their moral support and patience has borne fruit through completion of this thesis which will result in award of the prestigious degree of M.Tech in Materials Science & Engineering.

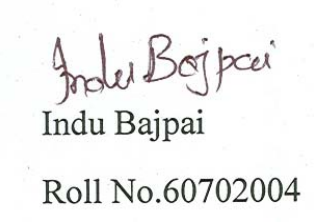

Indu Bajpai

Roll No.60702004

TABLE OF CONTENTS

List of abbreviations used

CNTs	Carbon nanotubes
MWNTs	Multiwall Carbon nanotubes
p-MWNTs	Pristine Multiwall Carbon nanotubes
c-MWNTs	Carboxylated Multiwall Carbon nanotubes
a-MWNTs	Acylated Multiwall Carbon nanotubes
f-MWNTs	Functionalized Multiwall Carbon nanotubes
GOD	Glucose oxidase enzyme
GOD-a-MWNTs	Glucose oxidase attached on Acylated Multiwall Carbon nanotubes
PBS	Phosphate buffer
PANI	Polyaniline
PANI/MWNTs	Multiwall Carbon nanotubes and polyaniline
PANI/a-MWNTs	Composite of polyaniline and acylated MWNTs
PANI/GOD-a-MWNTs	Composite of GOD attached on a-MWNTs and Polyaniline
CP	Conducting Polymer
FT-IR	Fourier Transform Infra-red (FT-IR) Spectroscopy
FE- SEM	Field Emission scanning electron microscopy
ITO	Indium Tin Oxide
POD	Peroxidase

ABSTRACT

Carbon Nanotubes (CNTs) are 1D structure, consisting of cylindrical graphite sheets with nanometer diameter and large aspect ratio. They have attracted enormous interest over past number of years due to their excellent electrical, mechanical and chemical properties. The combination of biological molecules and CNTs is of great importance in the process of developing new nano-scale devices for future biological, medical and electronic applications.

Glucose oxidase (GOD) is a flavin enzyme used commercially on massive scale to monitor blood glucose level in diabetics. The GOD enzyme can be attached to MWNTs and can be reversibly oxidized without complete loss of enzymatic activity. The present thesis work is concentrated on the functionalization of MWNTs (f-MWNTs), attachment of GOD on f-MWNTs, GOD activity in GOD-MWNTs composites at different time intervals and finally fabrication of enzyme electrode. GOD is attached with acylated MWNTs (a-MWNTs). The functionalization of MWNTs and the attachment of enzyme to MWNTs were carried out by chemical route and it was further characterized by FT-IR and FE-SEM techniques.

Enzyme activity is an important aspect for the development of biosensor. During this work, the activity measurements were carried out with UV-Visible spectrophotometer using SIGMA standard procedure. The results conclude that GOD retained its activity even after immobilization on f-MWNTs. Every week (maximum up to 8 weeks), the experiments related to the measurement of enzyme activity was repeated and GOD in GOD-MWNTs composite was again found active.

Conducting polymers are highly flexible in their chemical structure and redox characteristics. The composite of polyaniline and MWNTs was prepared by electrochemical technique on ITO coated glass plates. These composites were characterized by FT-IR and Cyclic Voltammetry techniques. The peak shift in the cyclic voltammogram of these composites, revealed the functionalization of MWNTs, attachment of GOD to f-MWNTs and formation of PANI/ GOD-a-MWNTs composite.

CHAPTER-1
INTRODUCTION

1.1 Carbon nanotubes

The carbon nanotubes (CNT) were discovered in 1976 when Endo synthesized vapor-grown carbon fibers, however at the time, it was not given any thought and focus [1]. In 1991, Iijima and his coworkers discovered multi-walled carbon nanotubes (MWNT) shown in figure (1.1). In 1993, Iijima and Bethune discovered single-walled carbon nanotubes (SWNT) [2].

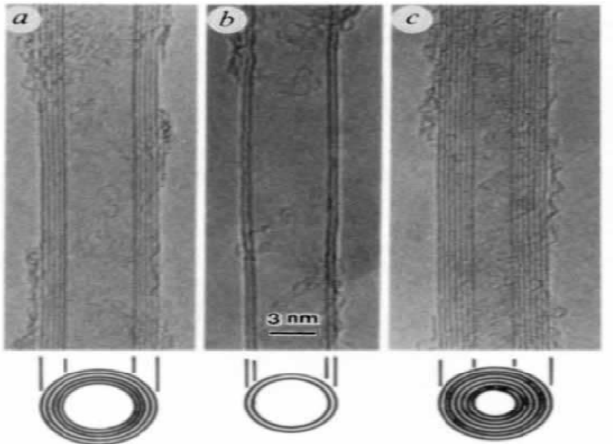

Fig 1.1: Electron micrograph of microtubes of graphitic carbon [this figure is adapted from Iijima, Sumio, "Helical microtubules of graphitic carbon" Nature. 1991]

1.1.1 Types of carbon nanotubes

Basically, there are two groups of carbon nanotubes, multiwall (MWNTs) and single-wall (SWNTs) carbon nanotubes [3]. An individual SWNT can be visualized as a single graphite sheet rolled into a tube and caped by two hemispheric fullerenes. MWNTs, can be visualized as concentric and closed graphite tubules with multiple layers of graphite sheets that define a hole typically from 2 to 25 nm separated by a distance of approximately 0.34 nm [2,3]. Bonding in CNTs is essentially sp^2; the circular curvature

causes σ bonds to be slightly out of plane, the π orbital is more delocalized outside the tube [1].

1.1.2 Structures of Carbon Nanotubes

The unique structure of CNTs leads to a number of unusual properties in these materials. MWNTs are regarded as metallic conductors. SWNTs are a mixture of metallic and semiconducting material, depending sensitively on their geometrical structure [4].

Atomic structure of nanotubes can be described in terms of tube chirality, or helicity, which is defined by the chiral vector, C_h and the chiral angle, θ [2]. A SWNT can be viewed as graphite sheet rolled up into a seamless cylinder. There are several ways to roll it. Therefore, different types of tubes can be formed. A carbon nanotube has a rolling direction expressed by the chiral vector C_h.

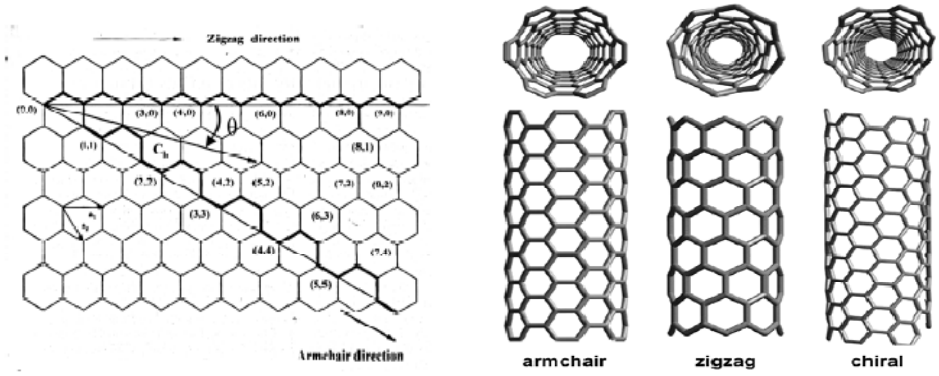

Fig 1.2: the graphene sheet and Structures of CNTs

Two unitary vectors a_1 and a_2 are necessary to determine the rolling direction, and $C_h = na_1 + ma_2$ - (n, m), which is often described by the pair of indices (n, m) that denote the number of unit vectors na_1 and ma_2 in the hexagonal honeycomb lattice contained in the vector C_h as shown in Figure 1.2. For a graphite sheet rolled up in a zigzag or a_1 direction, the axis of the zigzag nanotube corresponds to $\theta = 0^0$. Zigzag tubes are semiconducting. The so-called armchair nanotube is attained by rolling up the graphite sheet in the armchair direction. The axis in the armchair CNTs corresponds to $\theta = 30^0$

which gives to metallic tubes. The nanotube axis for so-called chiral nanotubes corresponds to $0^0 \langle \theta \langle 30^0$. They are semiconducting nanotubes [5].

1.1.3 Properties of Carbon Nanotubes

CNTs exhibit extraordinary properties, of which the most outstanding are summarized in Table 1.1. In mechanical properties, they are stiffer than any other material and about 100 times the strength of steel [5]. The properties of nanotubes will be influenced by the presence of defect sites on the walls and at the ends of the nanotube [6]. CNTs show good load transfer characteristics with metal matrix composite [7]. Particularly, SWNTs have demonstrated exciting optical phenomena, such as luminescence (fluorescence), ultra-fast switching response, polarization effect and the antenna length effect (in the low wavelength region)[5]. The dielectric responses of the carbon nanotubes are found to be highly anisotropic. Owing to their nearly one dimensional electronic structure, the electronic transport in metallic SWNTs and MWNTs occurs ballistically (without scattering) over long lengths which enables nanotubes to carry high currents with negligible heating [7].

Carbon nanotubes are low in weight, have high strength and a high aspect ratio (long length compared to a small diameter), and because of these properties are considered to be the ultimate in carbon fibers [8]. Carbon nanotubes have amazing electrical properties. These properties include metallic or semiconductor conductance, ballistic conductance, quantized conductance and very high current densities. The electronic properties of the carbon nanotubes are very sensitive to their structure.

The electrical and electronic properties of nanotubes are affected by distortions like bending and twisting. Although graphite is a zero-gap semiconductor, theory has predicted that carbon nanotubes can be either metals or semiconductors with different size energy gaps, depending very sensitively on the diameter and helicity of the tubes [7]. Carbon nanotubes (CNTs) have many distinct properties that may be exploited to develop next generation of sensors. CNTs can be used as filters for filtration of bacterial

contaminants such as Escherichia coli from water and heavy hydrocarbons from petroleum because of their exceptional thermal and mechanical stability and high surface area [7]. Some other applications of CNTs are Energy storage devices, electrochemical super capacitors, field emitting devices, transistors and nano probes and sensors [9].

Table 1.1 Properties of carbon nanotubes

Parameter	**Values and Units**	**Observations**
Length of unit vector	$A=\sqrt{3}a_{c-c}= 2.49A^0$	$a_{c-c}= 1.44A^0$ is the carbon bond length
Current Density	$>10^9 A/cm^2$	1000 time larger than the current density of Copper
Young modulus	1Tpa	Many order of magnitude stronger then the steel
Thermal conductivity	6600W/Mk	More thermally conductive than most crystals
Mobility	10,000 – 50,000 $cm^2V^{-1}s^{-1}$	Simulations indicate mobilities beyond 100,0000 $cm^2V^{-1}s^{-1}$
Mean free path	300-700nm semiconducting CNT 1000-3000nm Metallic CNTs	-Measured at room temperature - At least three times larger than the best semiconducting hetero-structures
Conduction in ballistic transport Luttinger parameters g	$G=4e^2/h=155\mu S$ $1/G=6.5k$ 0.22	
Orbital magnetic moment	0.7 $meVT^{-1}$(d=2.6nm) 1.5$meVT^{-1}$(d=5nm)	The electrons are strongly correlated in CNTs. The orbital magnetic moment depends on the tube diameter.

1.2 Conducting Polymers

Until about 30 years ago all carbon based polymers were rigidly regarded as insulators. The idea that plastics could be made to conduct electricity would have been considered to be absurd. Polymers were utilized as inactive packaging and insulating material. This very narrow perspective is rapidly changing as a new class of polymer known as intrinsically conductive polymer or electro active polymers are being discovered. Although this class is in its infancy, much like the plastic industry was in the 30's and 50's, the potential uses of these are quite significant. In 1958, polyacetylene was first synthesized by Natta et al. as a black powder. This was found to be a semi-conductor with conductivity between 7 x 10^{-11} to 7 x 10^{-3} Sm^{-1}, depending upon how the polymer was processed and manipulated. This compound remained a scientific curiosity until 1967, when a postgraduate student of Hideki Shirakawa at the Tokyo Institute of Technology was attempting to synthesis polyacetylene, and a silvery thin film was produced as a result of a mistake [10].

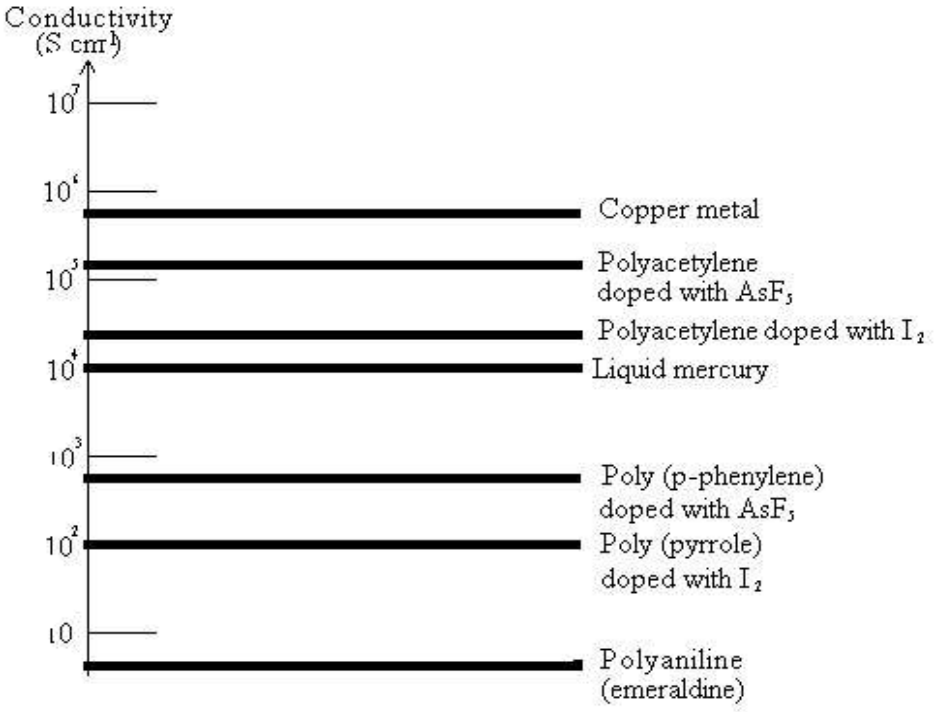

Fig 1.3 Conductivity comparison curve of polymers and metals

Conductivity of Polyaniline (PANI) is about 8 Scm^{-1}. Polyaniline has four basic states that are leucoemeraldine base (fully reduced form), emeraldine (only conducting) pernigraniline (fully oxidized) [7].

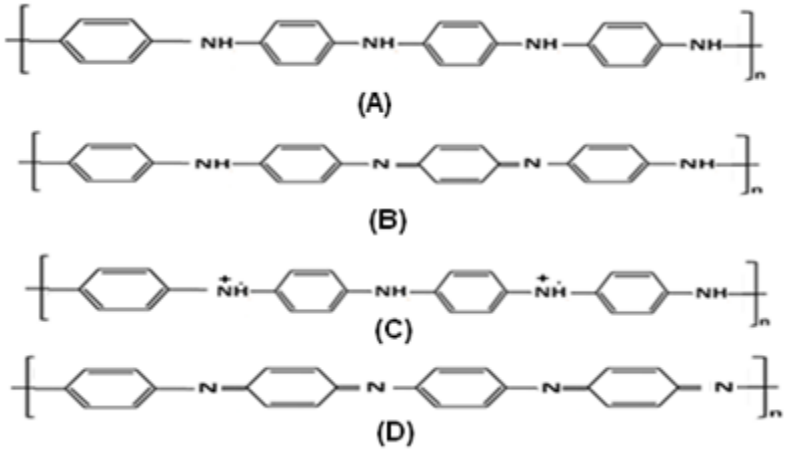

Fig 1.4 Different redox forms of Polyaniline: (a) leucoemeraldine base (reduced form), (b) emeraldine base (half-oxidized form), (c) conducting emeraldine salt (half-oxidized and protonated form), and (d) pernigraniline base (fully oxidized form).

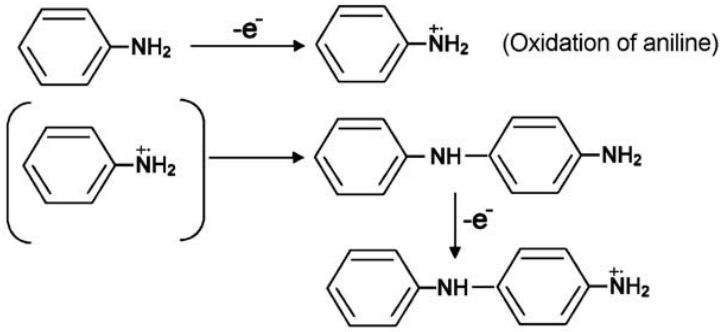

Fig 1.5: Polymerization mechanism of aniline

Polyacetylene, polyphenylene, polyphenylene vinylene, Polyaniline, Polypyrrole and polythiophene are some example of conducting polymers. It has been found that about a dozen different polymers and polymer derivatives undergo to transition when doped with a weak oxidation agent or reducing agent. They are all various conjugated polymers. This early work has led to an understanding of the mechanisms of charge storage and charge transfer in these systems. All have a highly conjugated electronic state. This also causes the main problems with the use of these systems, that of processibility and stability. Most early conjugated polymers were unstable in air and were not capable of being processed.

The most recent research in this has been the development of highly conducting polymers with good stability and acceptable processing attributes [10].

1.2.1 Charge Transport

Conductive polymers are peculiar in that they conduct current without having a partially empty or partially filled band. Their electrical conductivity cannot be explained well by simple band theory. For example, simple band theory cannot be used to explain why the charge carriers, usually electrons or holes, in polyacetylene and polypyrrole are spin less. The electronic phenomena in these electronic polymers cannot be completely explained by using the theory of conventional inorganic semiconductors.

The mechanism of conduction and behavior of charge carriers in the conducting polymers have been explained using the concept of solitons, polarons and bipolarons. A radical cation that is partially delocalized over some polymer segment is called a **polaron**. It stabilizes itself by polarizing the medium around it. It is really a radical cation and has a spin of 1/2.

When an electron is removed from the top of the valence band of a conjugated polymer, a vacancy (hole or radical cation) is created that does not delocalize completely, as would be expected from classical band theory. Only partial delocalization occurs, extending over several monomeric units and causing them to deform structurally. The energy level associated with this radical cation represents a destabilized bonding orbital and thus has a higher energy than the energies in valence band. This rise in energy is similar to the rise in energy that takes place after an electron is removed from a filled bonding molecular orbital. If another electron now is removed from the already oxidized polymer containing the polaron, two things can happen: This electron could come from either a different segment of the polymer chain, thus creating another independent polaron, or from the first polaron level (remove the unpaired electron) to create a special dication, which is called a **bipolaron**. Low doping levels give rise to polarons, whereas higher doping levels produce bipolarons. Compared to polaron, bipolaron is doubly charged but spin

less. The bipolaron also has structural deformation associated with it. The two positive charges of the bipolaron are not independent, but act as a pair, much like the cooper pair in the Bardeen-Cooper-Schrieffer (BCS) theory of superconductivity. Both polarons and bipolarons are mobile and can move along the polymer chain by the rearrangement of double and single bonds in the conjugated system that occurs in an electric field. If many bipolarons are formed, say as a result of high doping, their energies can start overlapping at the edges, which creates narrow bipolaron bands in the band gap.

In polyacetylene, which has a degenerate ground state (two equivalent resonance forms), the bipolaron dissociates into two independent cations, which are spin less and are called **solitons**. Solitons do not form in polymers with nondegenerate ground state, such as polypyrrole, polythiophene and polyphenylene. These polymers are called nondegenerate because their resonance forms are not identical if they are superimposed. Doping with a suitable dopant can increase the concentration of charged solitons.

1.2.2 Stability of Conducting Polymers

Thermal stability of the most of the conducting polymers is poor excepting the heterocyclic polymers. The rate of thermal degradation is very much dependent on the environment. Polyacetylene, for example, degrades at room temperature in air or oxygen atmosphere, but in helium, its degradation starts only at 320^0C [11]. Similarly, polythiophene and its derivatives are stable up to 200^0 to 250^0C in air, but do not decompose up to 700^0C in inert atmosphere [12]. Nature of the dopant also affects the thermal stability of the polymers. Polypyridine, for example, doped with arylsulfonates is only stable up to 80^0C in humid environment, but when doped with BF_4^- it retains its stability up to 150^0C [13]. Incorporation of hetroatoms having non-bonding electron pairs in the conjugated chain structure increases the thermal stability in conducting polymers.

1.2.3 Processability

Conducting polymers possess poor processability. Due to extended conjugated chain structure, these polymers are insoluble and infusible and hence are not easily processable. Polyacetylene, for example, shows electrical conductivity in the semiconducting range. But on exposure to atmosphere its conductivity falls rapidly. A number of general techniques have been developed for improving the processability of conducting polymers. Block copolymerization, chain flexibility and Polymer blend [13].

Table 1.2 stability and processing attributes of some conducting polymers

POLYMER	**CONDUCTIVITY (Ω^{-1} cm^{-1})**	**STABILITY (doped state)**	**PROCESSING POSSIBILITIES**
Polyacetylene	10^3 - 10^5	Poor	Limited
Polyphenylene	1000	Poor	Limited
PPS	100	Poor	Excellent
PPV(Poly-p-phenylenevinylene)	1000	Poor	Limited
Polypyrrole	100	Good	Good
Polythiophenes	100	Good	Excellent
Polyacetylene	10	Good	Good
Polyaniline	8	Excellent	Excellent

1.2.4 Applications

There has been growing interest in CPs because of their wide range of potential application in the areas such as rechargeable batteries, gas separation membranes, EMI shielding, electro chromic display devices etc. The extended π-systems of conjugated polymer are highly susceptible to chemical or electrochemical oxidation or reduction. These alter the electrical and optical properties of the polymer, and by controlling this oxidation and reduction, it is possible to precisely control these properties. Since these

reactions are often reversible, it is possible to systematically control the electrical and optical properties with a great deal of precision. It is even possible to switch from a conducting state to an insulating state. [10].The conducting polymers have been widely used for the development of various biosensors [15]. Immobilization of enzyme in conducting polymer by electro synthesis is an attractive technique for fabricating enzyme electrode [16].

1.3 Composite of CNTs and Conducting Polymers

Composite are synthesized to get the material of improved properties. CNTs can be used as nano fillers and nano reinforcement for improving mechanical thermal and impact resistant properties of advance composite materials [17].

A main advantage of using nanotubes for structural polymer composites is that nanotube reinforcements will increase the toughness of the composites by absorbing energy during their highly flexible elastic behavior. Other advantages are the low density of the nanotubes, an increased electrical conduction and better performance during compressive load. Another possibility, which is an example of a non-structural application, is filling of photoactive polymers with nanotubes. PPV (Poly-p-phenylenevinylene) filled with MWNTs and SWNTs is a composite, which has been used for several experiments. These composites show a large increase in conductivity with only a little loss in photoluminescence and electro-luminescence yields. Another benefit is that the composite is more robust than the pure polymer [10].

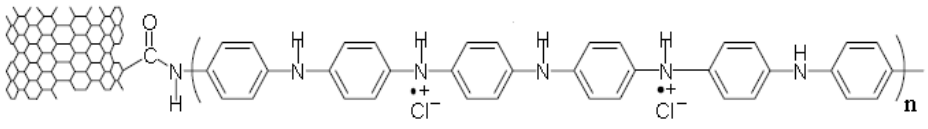

Fig 1.6: Composite of CNTs and conducting polymer

It was reported that PANI fiber containing CNTs show remarkable improvement in mechanical strength and conductivity. PANI and CNTs combination is excellent plate form electrochemical application [18]. Recent studies show that CNTs can be dissolved

in aniline via formation of doner acceptor complex. Composite PANI/CNTs can be prepared by mainly two ways, one includes sidewall grafting (linkage) and other non covalent mixing/adsorption (exohedral interaction).The non covalent approach includes surfactant modification, polymer wrapping or polymer adsorption. The main disadvantage of non covalent approach is that the force between the wrapping molecules and the CNTs are very weak due to slippage of stacked molecules. The covalent approach can be initiated by functionalization of CNTs with carboxylic acid group which increases the compatibility between CNTs and the matrix polymer by directly grafting polymer chains onto the surface of CNTs [19].

1.4 Biosensor

The history of biosensors started in the year 1962 with the development of enzyme electrodes by the scientist Leland C. Clark.

1.4.1 Definition

A commonly cited definition is: "a biosensor is a chemical sensing device in which a biologically derived recognition entity is coupled to a transducer to allow the quantitative development of some complex biochemical parameter", and also: "a biosensor is an analytical device which comprises of a specific biological element (that creates a recognition event) and a physical element (that transduces the recognition event)".

The basic operation of a biosensor can be illustrated with the help of Fig. 2.1. A specific "bio" element (say, enzyme) recognizes a specific analyte and the "sensor" element transduces the change in the biomolecules into an electrical signal. The bio element is very specific to the analyte to which it is sensitive. It does not recognize other analytes.

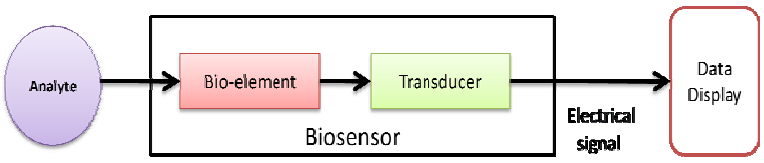

Fig. 1.7 Schematic diagram of biosensor

Depending on the transducing mechanism used, the biosensors can be of many types such as: (i) Resonant biosensors, (ii) Optical-Detection biosensors, (iii) Thermal-Detection biosensors, (iv) Ion-Sensitive FET (ISFET) biosensors, and (v) Electrochemical biosensors. Biosensors can have a variety of biomedical, industry, and military applications.

1.4.2 Basic Concepts

The "bio" and the "sensor" elements can be coupled together in one of the four possible: Membrane Entrapment, Physical Adsorption, Matrix Entrapment, and Covalent Bonding. In the **Membrane Entrapment** scheme, a semi permeable membrane separates the analyte and the bio element, and the sensor is attached to the bio element. The **Physical Adsorption** scheme is dependent on a combination of Van der Waals forces, hydrophobic forces, hydrogen bonds, and ionic forces to attach the biomaterial to the surface of the sensor. The **Porous Entrapment** schemes based on forming a porous encapsulation matrix around the biological material that helps in binding it to the sensor. In **Covalent Bonding** the sensor surface is treated as a reactive group to which the biological materials can bind. The typically used bio-element, enzyme is a large protein molecule that acts as a catalyst in chemical reactions, but remains unchanged at the end of reaction. An enzyme reacted with a substrate to forms a complex molecule which under appropriate conditions forms the desirable product molecule releasing the enzyme at the end. The enzymes are extremely specific in their action.

1.4.3 Electrochemical Biosensors

Electrochemical biosensors are mainly used for the detection of this class of biosensors is that many chemical reactions produce or consume ions or electrons which in turn cause some change in the electrical properties of the solution which can be sensed out and used as measuring parameter. Electrochemical biosensors can be classified based on the measuring electrical parameters as follows:

(A) Conductometric

The measured parameter is the electrical conductance/resistance of the solution. When electrochemical reactions produce ions or electrons, the overall conductivity or resistivity of the solution changes. This change is measured and calibrated to a proper scale. Conductance measurements have relatively low sensitivity. The electric field is generated using a sinusoidal voltage (AC) which helps in minimizing undesirable effects such as Faradaic processes, double layer charging and concentration polarization.

(B)Amperometric

This high sensitivity biosensor can detect electro active species present in biological test samples. Since the biological test samples may not be intrinsically electro-active, enzymes are needed to catalyze the production of radio-active species. In this case, the measured parameter is current.

(B)Potentiometric

In this type of sensor the measured parameter is oxidation or reduction potential of an electrochemical reaction. The working principle relies on the fact that when a ramp voltage is applied to an electrode in solution, a current flow occurs because of electrochemical reactions. The voltage at which these reactions occur indicates a particular reaction and particular species.

1.4.4 Glucose Biosensors

The main concept in glucose biosensor is glucose reacts with glucose oxidase (GOD) to form gluconic acid while producing two electrons and two protons, thus reducing GOD. The reduced GOD, surrounding oxygen, electrons and protons (produced above) react to form hydrogen peroxide and oxidized GOD (the original form). This GOD can again react with more glucose. The higher the glucose content, more oxygen is consumed. On

the other hand, lower glucose content results in more hydrogen peroxide. Hence, either the consumption of oxygen or the production of hydrogen peroxide can be detected by the help of platinum electrodes and this can serve as a measure for glucose concentration. The current and future applications of glucose biosensors are very broad due to their immediate use in diabetic self-monitoring of capillary blood glucose. These types of monitoring devices comprise one of the largest markets for biosensors today and their existence has dramatically improved the quality of life of diabetics [20].

The most typical part of electrochemical biosensors is the presence of a suitable enzyme in the biorecognition layer providing electro active substances for detection by the physico-chemical transducer providing the measurable signal [21].

1.5 Motivations

Glucose biosensor is very important for our society. This sensor is very useful for detection of glucose level in human body so that diabetic like diseases can be detected. The glucose oxidase (GOD) enzyme detects the glucose. So for the fabrication of glucose sensor the immobilization of GOD enzyme on any substrate is very essential and primary requirement for the electrochemical biosensor. A conducting substrate is needed which can easily detect and transfer the electrical signal. Now a day's CNTs and conducting polymers are very popular conducting materials for the device fabrication point of view. GOD enzyme can be immobilized on CNTs, conducting polymers and there composite.

MWNTs show fast response, high sensitivity and stability to glucose so MWNTs are good electrode material for biosensor [22]. The functionalization and chemical modification of carbon nanotubes forces the utilization of carbon nanotubes for various nano materials like enzyme for biosensing interface [23, 24, 25]. Glucose biosensor based on nanotubes was found to be suitable for detection of glucose [26, 27].

Doping of CNTs in PANI greatly influences the conductivity of composite [16, 28]. PPy (Polypyrrole) coated CNTs exhibit improved electrochemical redox performance [4]. Conducting PANI-PVS having amine functional group can be utilized as a suitable matrix for the cross-linking of GOD [29].

But the limited life time of a biosensor sensor is still a problem. This problem could be resolved by modifying the processing conditions of CNT-PANI composite based biosensors. Keeping this aspect in point of view, the aim of studies presented in this thesis is mentioned in the subsequent section.

1.6 Aim of thesis

Aim of the work presented in this thesis is based on the modification of processing condition in order to get better life time of CNT-PANI based biosensors. Therefore, this work is aimed at

1. The covalent functionalization of MWNTs for the attachment of glucose oxidase.

2. The activity measurement of GOD attached on MWNTs.

3. The fabrication of PANI/GOD-MWNTs electrode for the investigation of electrochemical properties.

CHAPTER -2
EXPERIMANTAL DETAILS

This chapter presents the details of the modification of MWNTs via chemical treatment and attachment of enzyme on them. The experimental details include the functionalization of MWNTs, attachment of GOD enzyme on MWNTs, activity measurement of GOD modified MWNTs and the synthesis of PANI/GOD-MWNTs composite based electrodes. They are described in subsequent sections:

2.1. Functionalization of MWNTs

Functionalization of CNTs is an essential step for application point of view. The following steps were used with MWNTs:

2.1.1 Carboxylation

50 mg MWNTs were dispersed by sonicating in solution of HNO_3 and H_2SO_4 (1:3) for 2Hrs. Then 10 ml 1M HCl was added and solution was further sonicated for 30 min. After sonication solution was diluted with distilled water and then it was filtered by hydrophilic filter paper and washed with distilled water. Carboxylated MWNTs were dried under vacuum at 50^0 C. The powder of c-MWNTs was stored at room temperature [21].

Characterization

- 1mg powder was used for FT-IR characterization.

2.1.2 Acylation

Carboxylated MWNTs were dispersed by sonicating in solution of 1ml DMF and 20 ml $SOCl_2$ for 30 min. Then solution was stirred and refluxed at 80^0C for 24 Hrs. After that solution was filtered by hydrophobic filter paper and washed by THF. The acylated MWNTs were dried under vacuum at room temperature [21].

Characterization

- 1mg powder was used for FT-IR characterization.

2.2 GOD attachment on a-MWNTs

20 mg acylated MWNTs were dispersed by sonicating in 20 ml PBS buffer (pH 6.8) for 30 min. 10 mg GOD were dissolved in 10ml PBS buffer (pH 6.8). These two solutions were mixed in each other and the solution was kept at 37^0 C for 5 days in incubation chamber.

After 5 days solution was filtered with hydrophilic filter paper and GOD- a-MWNTs were washed with deionized water and dried under vacuum at 25 ^{0}C.

For activity measurement GOD-a-MWNTs were washed with deionized water and then stored in sodium acetate buffer (pH 5.1).

For Cyclic Voltammetry measurements solution was washed with PBS buffer (pH 6.8) and stored in PBS buffer (pH 6.8). All solutions and powder were stored at 4^0C.

Characterization

- 1mg powder was used for FT-IR characterization.
- 0.1mg a-MWNTs were dispersed in 1ml deionized water and sample was prepared for FE-SEM characterization.
- 1 ml solution of GOD- a-MWNTs was used for electrochemical analysis.

2.3 Measurement of activity of immobilized enzyme
(Enzymatic Assay of GLUCOSE OXIDASE (EC 1.1.3.4) Sigma

Glucose oxidase (GOD) catalyzes the oxidation of β-D-glucose to D-glucono-δ-lactone and hydrogen peroxide. It is highly specific for β-D-glucose and does not act on α-D-glucose.

Principle

Glucose oxidase catalyses the oxidation of β-D-glucose to D-glucono- δ-lactone with the concurrent release of hydrogen peroxide.

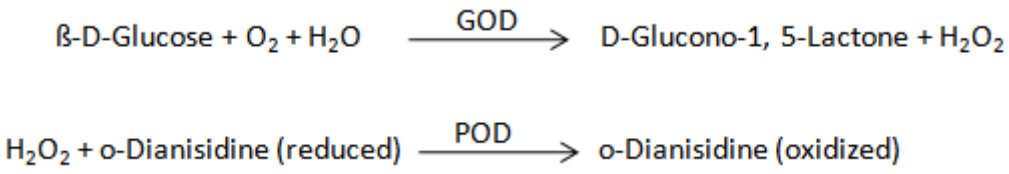

Abbreviations used:

GOD = Glucose Oxidase

POD = Peroxidase

Conditions: T = 35^0C, pH = 5.1, A_{500nm}, Light path = 1 cm

METHOD: Continuous Spectrophotometric Rate Determination

Procedure:

The activity measurements for GOD and GOD immobilized on a-MWNTs was carried out by a spectrophotometric method (sigma). The reaction mixture consisted of glucose (2.4 mL; 10 % w/v) and o-dianisidine (0.5 mL) in a sodium acetate buffer (0.05 M, pH 5.1) in the presence of horseradish peroxidase (0.1 mL) and GOD-a-MWNTs solution (0.1 mL) was added in test and sodium acetate buffer (0.1 mL) was added in blank. Both solutions were incubated for 20 min at room temperature and at 500nm, in spectrophotometer and the color was monitored.

The apparent enzyme (GOD) activity immobilized on a-MWNTs was estimated with following formula:

$$\text{Units/ml enzyme} = \frac{(\Delta A_{500nm}/\text{min Test} - \Delta A_{500nm}/\text{min Blank})\ (3.1)\ (df)}{(7.5)\ (0.1)}$$

Where,

3.1 = Volume (in milliliters) of assay

df = Dilution factor

7.5 = Millimolar extinction coefficient of oxidized o-Dianisidine at 500 nm

0.1 = Volume (in milliliters) of enzyme use

2.4 Fabrication of electrodes

First of all ITO coated glass plates were properly cleaned by acetone and aniline was distilled. Size of ITO plates is 1.5×1.0 cm^2. Electrodes were fabricated by cyclic Voltammetry mode and potentiostatic mode. ITO plate, platinum electrode and saturated calomel electrode (SCE) were used as working electrode, counter electrode and reference electrode respectively. The different types of fabricated electrodes are discussed below:

2.4.1 Fabrication of PANI electrode in 1M HCl

0.1 ml aniline was mixed in 6 ml HCl solution. The HCl solution works as an electrolyte. The 10 cycles were set in CV setup in voltage range 0.4V to 1.4V keeping scan rate of 10 mV/sec. The film was deposited on ITO plate. Resulting film was dried under vacuum at room temperature. Dried film was washed with deionized water to remove the HCl from the film and film was again dried under vacuum. Washing of film was performed twice.

2.4.2 Fabrication of PANI electrode in buffer

0.1 ml aniline was mixed in 6 ml PBS buffer (0.1M pH 6.8). The PBS solution works as an electrolyte. Film was deposited for 3min on ITO plate in potentiostatic mode at 2V. Resulting film was dried under vacuum at room temperature. Dried film was washed with deionized water to remove the buffer from the film and film was again dried under vacuum. Washing of film was performed twice.

Characterization

- Cyclic Voltammetry of the film was taken in voltage range from -0.15V to1.2V at scan rate of 10 mV/sec.

2.4.3 Fabrication of PANI / a- MWNTs composite electrode in buffer

1mg a-MWNTs were dispersed by sonicating in 6 ml PBS buffer (0.1M pH 6.8) for 1Hr. The 0.1ml aniline was mixed in above solution. Film was deposited for 3 min on ITO plate in potentiostatic mode at 2V. Resulting film was dried under vacuum at room temperature. Dried film was washed with deionized water to remove the buffer from the film and film was again dried under vacuum. Washing of film was performed twice.

Characterization

- Cyclic Voltammetry of the film was taken in voltage range from -0.5V to1.2V at scan rate of 10 mV/Sec.
- The film was characterized by FT-IR.

2.4.4 Fabrication of PANI / GOD- a-MWNTs composite electrode in buffer

1.0 ml solution of GOD- a-MWNTs was mixed in 6 ml PBS buffer (0.1M pH 6.8) and the solution was sonicated for 10 min. The 0.1ml aniline was mixed in above solution. PBS works as an electrolyte. Film was deposited for 3min on ITO plate in potentiostatic mode at 2.0 V. Resulting film was dried under vacuum at room temperature. Dried film was washed with deionized water to remove the buffer from the film and film was again dried under vacuum. Washing of film was performed twice. The film was stored at 4^0C.

Characterization

- Cyclic Voltammetry of the film was taken in voltage range from -0.2V to1.6V at scan rate of 10 mV/sec.
- The film was characterized by FT-IR.

CHAPTER-3

RESULTS AND DISCUSSION

The spectroscopic characterization of the MWNTs and MWNTs-polymeric samples is usually carried out by either preparing a thin film or making a solution of the polymer transparent to the incident radiation. In case of powders, a few mg is mixed with potassium bromide (KBr) in form of pellets to use for IR studies. UV-visible spectra give the energy band gap and defects states, while IR spectroscopy identifies and confirms the structure and presence of various groups on MWNTs and various linkage in MWNT-polymer composites. This is a very important characterization technique, especially when substitution, cross-linking and copolymerization are involved. Morphological information of materials has been taken from FE-SEM. The FE-SEM, FT-IR and Cyclic-Voltammetry characterizations are shown below:

3.1 FT-IR Results

The IR studies have been carried out for determining the functional group and molecular structure of the MWNTs, GOD-a-MWNTs, PANI, PANI/a-MWNTs, and PANI/GOD-a-MWNTs composites. The results of these studies are explained in the following sections.

3.1.1 FT-IR study of pristine MWNTs

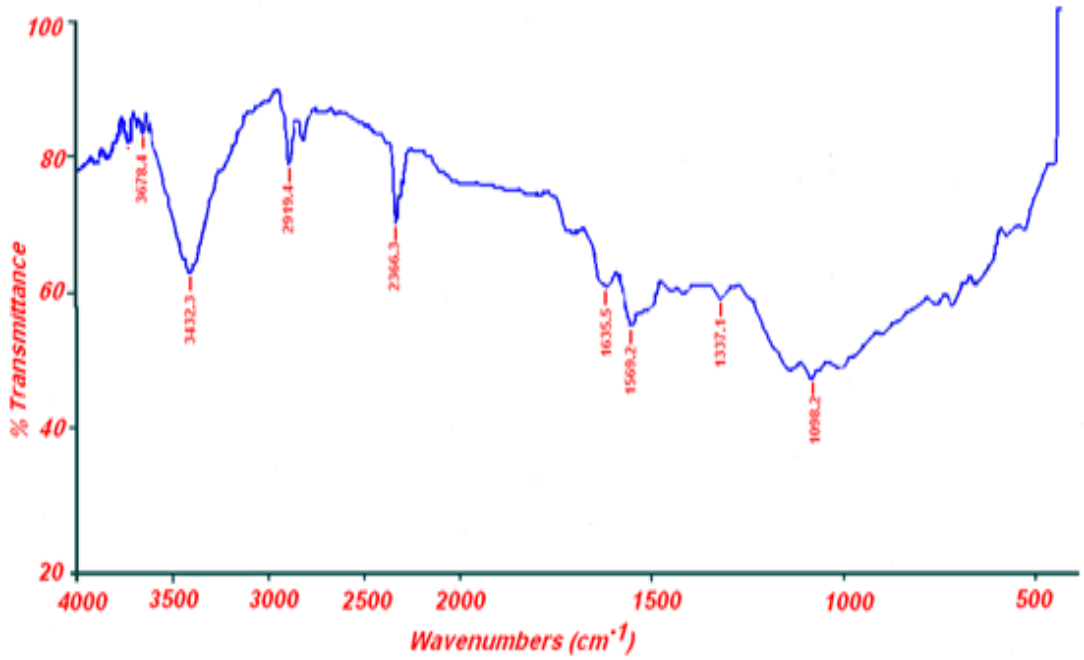

Fig 3.1: IR spectrum of pristine MWNTs

Fig 3.1 shows the IR spectra of pristine MWNTs. In this spectra various peaks were found but the main characteristic peaks were obtained at 3432.3 cm^{-1}, 2919.4 cm^{-1}, 2366.3 cm^{-1},1635.5 cm^{-1}, 1569.2 cm^{-1},1337.1 cm^{-1} and 1098.2 cm^{-1}. The peak at 3432.3 cm^{-1} was found due to OH group. The peak of C≡C bond in MWNTs was found at 2919.4 cm^{-1}. The peak at 2366.3 cm^{-1} was obtained due to CO_2 coating of IR optics. The peak at 1635.5 cm^{-1} arises due to C=C bond in MWNTs. The peak obtained at 1569.2 cm^{-1}, 1337.1 cm^{-1} and 1098.2 cm^{-1} occurs due to conjugated C=C bond in MWNTs, C=C bond stretching and C-C bond in MWNTs respectively.

The IR spectra of MWNTs obtained, corresponds to the vibrational stretching and bending of the bonds present in the various bonds of MWNTs.

3.1.2 FT-IR study of GOD

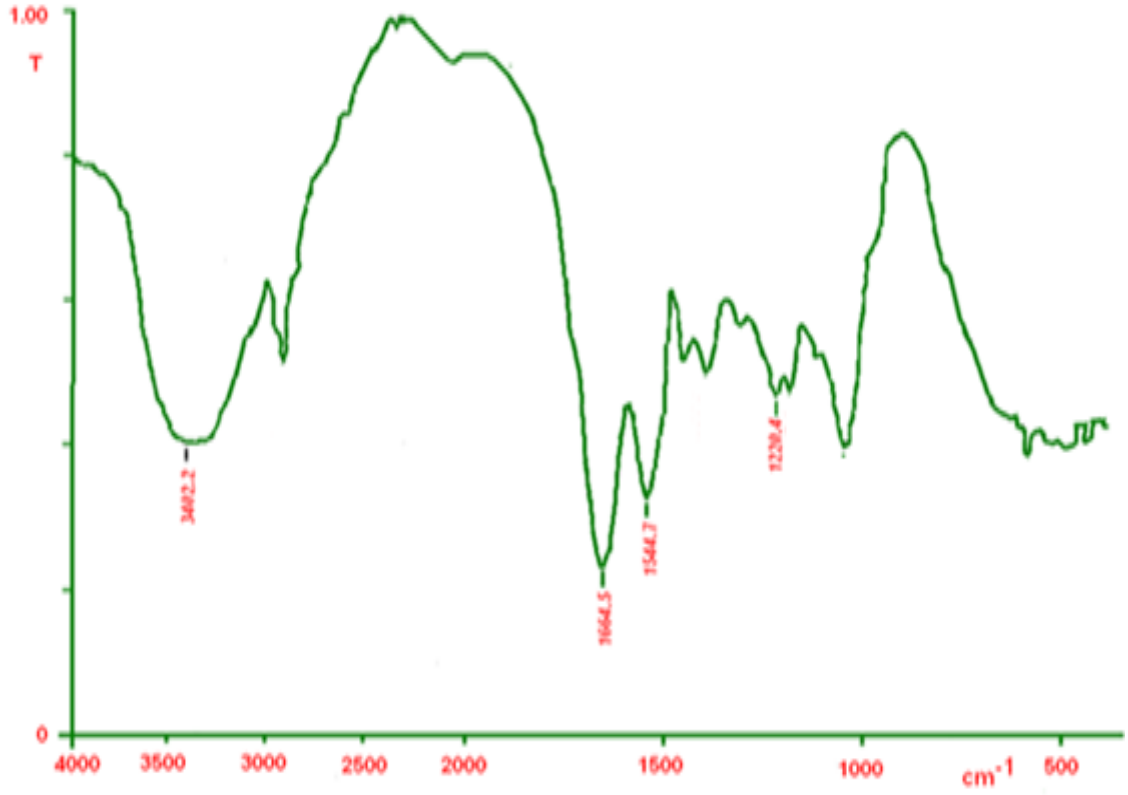

Fig 3.2: IR spectra of glucose oxidase

The IR spectrum of glucose oxidase was recorded in wave number range of 4000 cm^{-1} to 500 cm^{-1}. Various peaks were found in spectra but the main characteristic peaks were obtained at 3402.2 cm^{-1}, 2927.4 cm^{-1}, 1654.5 cm^{-1}, 1544.7 cm^{-1} and 1220.4 cm^{-1}. The peak at 3402.2 cm^{-1} was found due to N-H stretching vibration. The peak of C-H stretching vibration was found at 2927.4 cm^{-1}. The peak at 1654.5 cm^{-1} was obtained due to presence of amide I band. The peak at 1544.7 cm^{-1} arises due to presence of amide II band. The peak obtained at 1220.4 cm^{-1} occurs because of C-N stretching. The IR spectra for the enzyme GOD, corresponds to the bonds present in the molecules of enzyme (structural) which is being used as a control for the study of the IR spectra obtained for the acylated MWNTs. The various peaks seen here should not be present in enzyme attached MWNTs IR spectra.

3.1.3 FT-IR study of carboxylated MWNTs

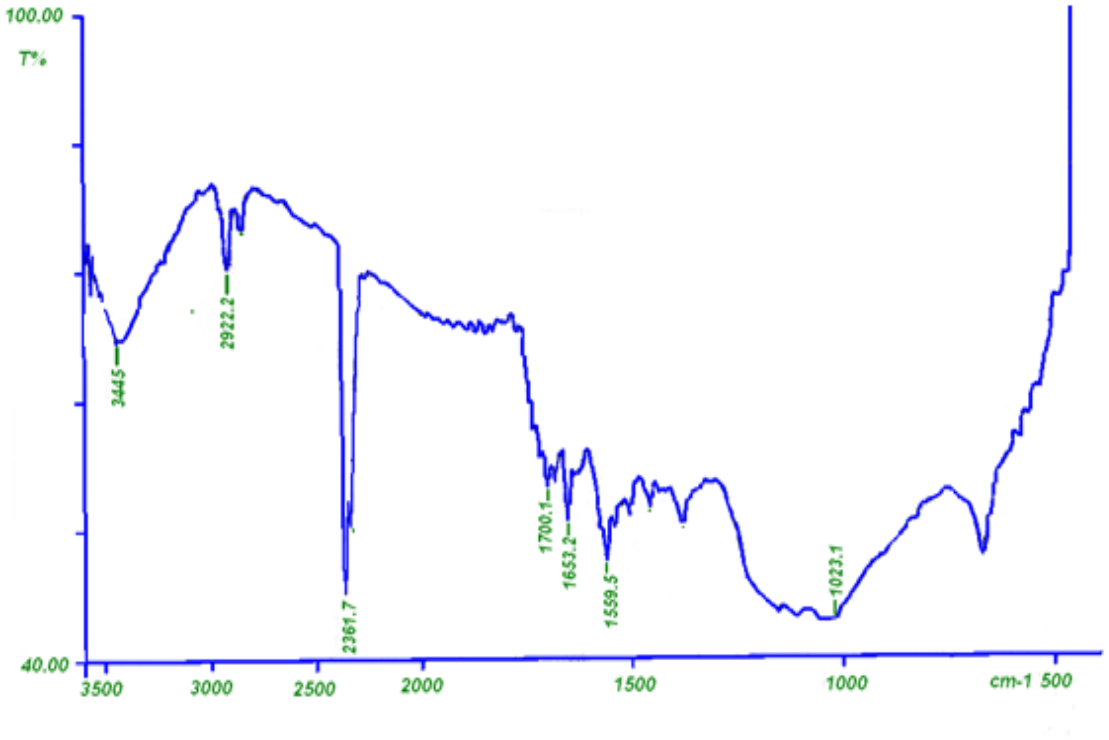

Fig 3.3: IR spectra of c-MWNTs

Fig 3.3 shows the IR spectra of carboxylated MWNTs. Various peaks were found in this spectra but the main characteristic peaks were obtained at 3445.0 cm^{-1}, 2922.2 cm^{-1}, 2361.7 cm^{-1}, 1700.1 cm-^{1}, 1653.2 cm^{-1}, 1569.5 cm^{-1} and 1023.1 cm^{-1}. The peak at 3445 cm^{-1} was found due to OH group of carboxylic acid. The peak of C≡C bond in MWNTs was found at 2922.2 cm^{-1}. The peak at 2361.7 cm^{-1} was obtained due to CO_2 coating of IR optics.

The peak at **1700.1 cm^{-1}** is the characteristic peak of **COOH** group in MWNTs. The peak obtained at 1653.2 cm^{-1} ,1569.5 cm^{-1}, and 1023.1 cm^{-1} occurs due to C=O stretching peak, carboxylic ion COO^- and C-O stretch in carboxylic acid in MWNTs respectively. The IR spectra of MWNTs obtained, corresponds to the vibrational stretching and bending of the bonds present in the various bonds of MWNTs. There are no characteristic peaks for any of the functional group.

3.1.4 FT-IR study of acylated MWNTs

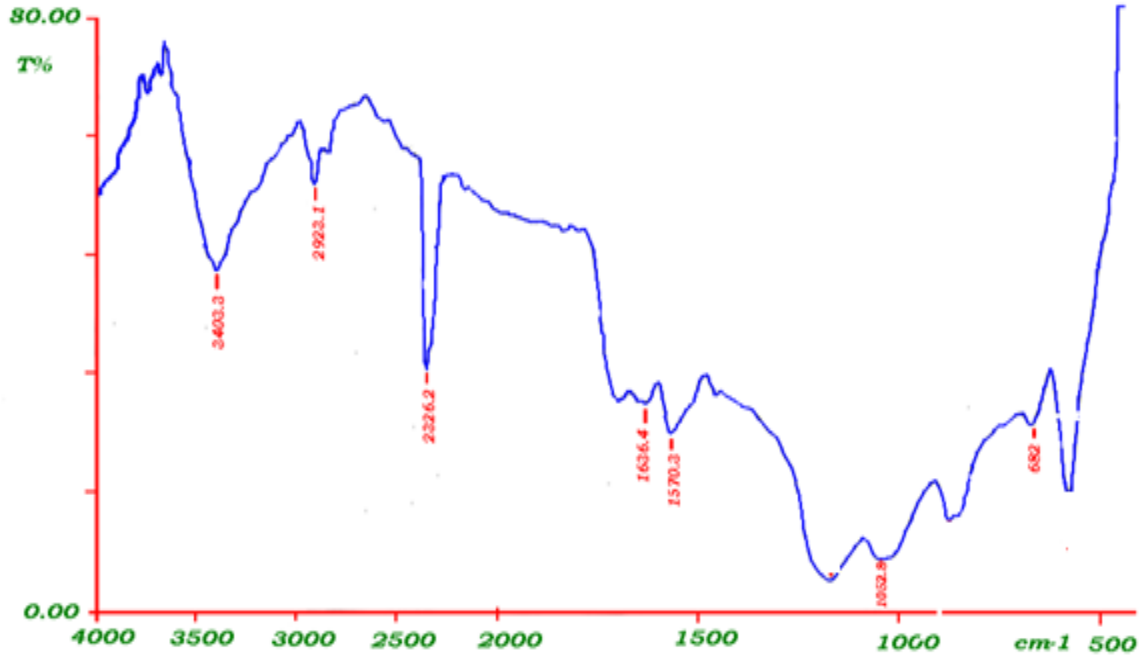

Fig 3.4: IR spectra of acylated MWNTs

Fig 3.4 shows the IR spectra of acylated MWNTs recorded in the voltage range from 4000 to 500 cm^{-1}. Various peaks were found in this spectrum but the main characteristic peaks were obtained at 3403.3 cm^{-1}, 2923.1 cm^{-1}, 2360.2 cm^{-1}, 1636.4 cm^{1}, 1570.3 cm^{-1}, 1052.8 cm^{-1} and 682.0 cm^{-1}. The peak at 3403.3 cm^{-1} was found due to OH group of carboxylic acid. The peak of C≡C bond in MWNTs was found at 2923.1 cm^{-1}. The peak at 2360.2 cm^{-1} was obtained due to CO_2 coating of IR optics.

The peak obtained at **1636.4 cm^{-1}** ,1570.3 cm^{-1}, and 1052.8 cm^{-1} occurs due to **C=O** stretching peak of COCl, carboxylic ion COO^- and C-O stretch in carboxylic acid in MWNTs respectively.. The peaks appear at **682.0 cm^{-1}** corresponds to the **C-Cl** group which appears generally in the range of 600 to 800 cm^{-1}. The IR spectra of a-MWNTs obtained, corresponds to the vibrational stretching and bending of the bonds present in the various bonds of MWNTs. These peaks obtained in the above spectrum corresponds to the stretching and bending been created in the MWNTs structure due to acylation of MWNTs.

3.1.5 FT-IR study of GOD-a-MWNTs

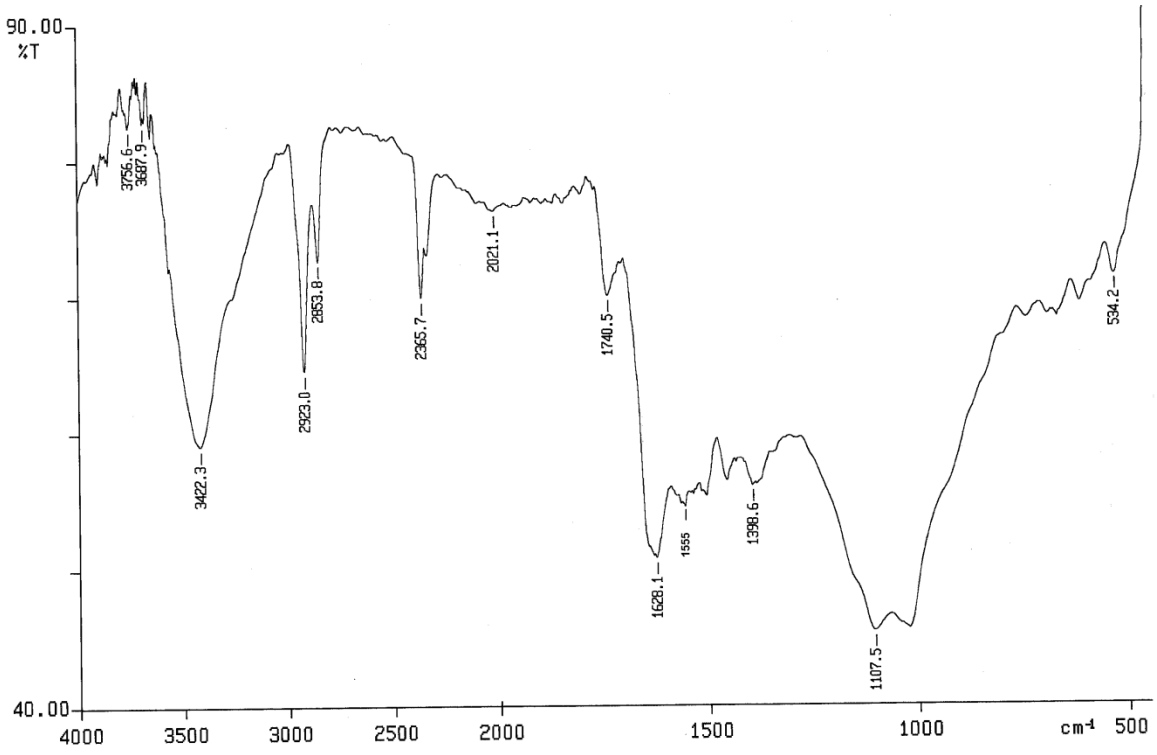

Fig 3.5: IR spectra of GOD-a-MWNTs.

Various peaks were found in this spectra but the main characteristic peaks were obtained at 3422.3 cm^{-1}, 2923.0 cm^{-1}, 2365.7 cm^{-1} , 1740.5 cm^{-1}, 1628.1 cm^{1}, 1555.0 cm^{-1} and 1398.6 cm^{-1}. The peak at 3422.3 cm^{-1} was found due to OH group of carboxylic acid. The peak of C-H bond in MWNTs was found at 2923.0 cm^{-1}.

The peak at 2365.7 cm^{-1} was obtained due to CO_2 coating of IR optics. The peak obtained at 1740.5 cm^{-1},**1628.1 cm^{-1}**, **1555.0 cm^{-1}**, and 1398.6 cm^{-1} occurs due to C=O stretching, vibration of **amide I,** vibration of **amide II** and due to presence of nitro group ($-NO_2$) respectively. The peak near 1020 cm^{-1} arises due to C-N stretch. These peaks obtained in the above spectrum correspond to the stretching and bending being created in the MWNTs structure due to the functionalization by the enzyme group.

3.1.6 FT-IR Study of Polyaniline

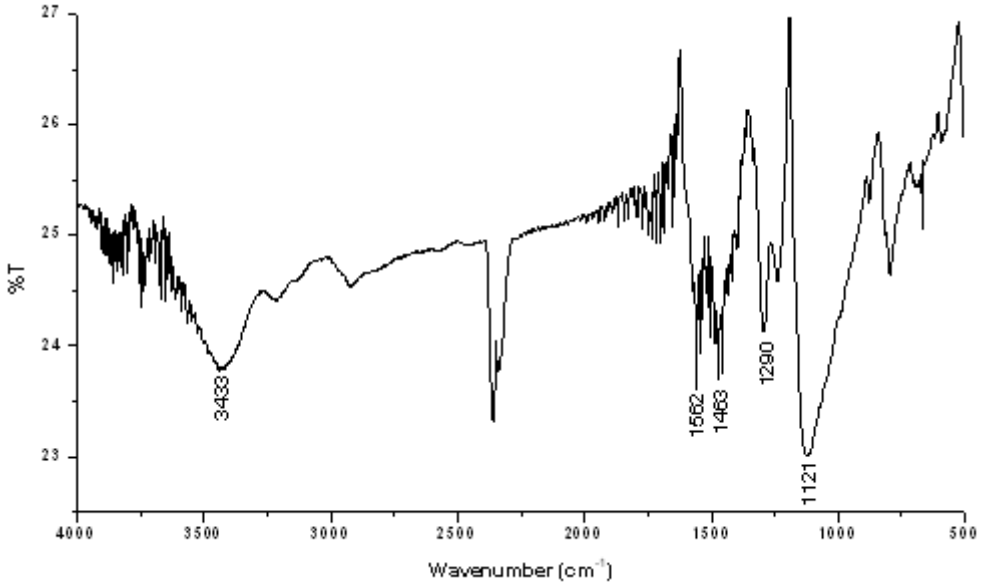

Fig 3.6: IR spectra of PANI

Fig 3.6 shows the IR spectra of PANI recorded between the wave number rang of 500 to 4000 cm^{-1}. The presence of benzoid ring vibration was obtained at 1463 cm^{-1}. The quinoid ring vibration was found at 1562 cm^{-1}.

The strong band around 1121 cm^{-1} is the characteristic peak of PANI conductivity and is a measure of the degree of the delocalization of electrons. The peak around 3433 cm^{-1} is assigned to the N-H stretching mode.

3.1.7 FT-IR Study of a-MWNT/PANI composite

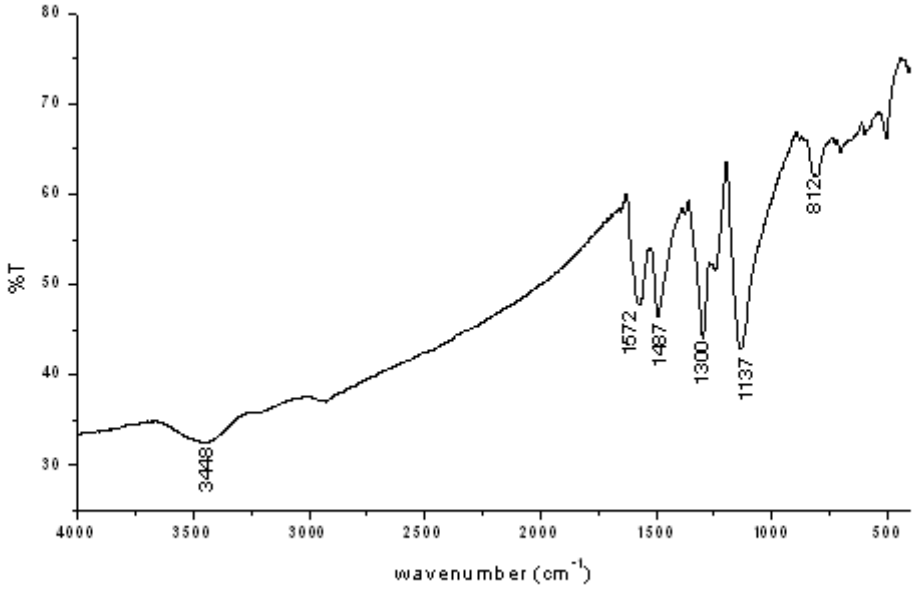

Fig 3.7: IR spectra of PANI/ a-MWNTs composite

The IR spectra of PANI/a-MWNTs shown above was recorded between the wave number rang of 500 to 4000 cm^{-1}**.** There were clear differences between this and the spectrum of PANI (Fig.3.6). The **N-H stretching region** near **3448.0 cm^{-1}** showed broad peak.

The shift in peak observed as follows:

1. from 3433.0 cm^{-1} to 3448.0 cm^{-1}
2. from 1463.0 cm^{-1} to 1487.0 cm^{-1}
3. from 1562.0 cm^{-1} to 1572.0 cm^{-1}
4. from 1121 cm^{-1} to 1137cm^{-1}.

The shift in peaks indicates the some interaction between MWNTs and PANI during composite formation electrochemically. This confirms the formation of a-MWNT/PANI composite.

3.1.8 FT-IR Study of GOD attached MWNTs/PANI composite

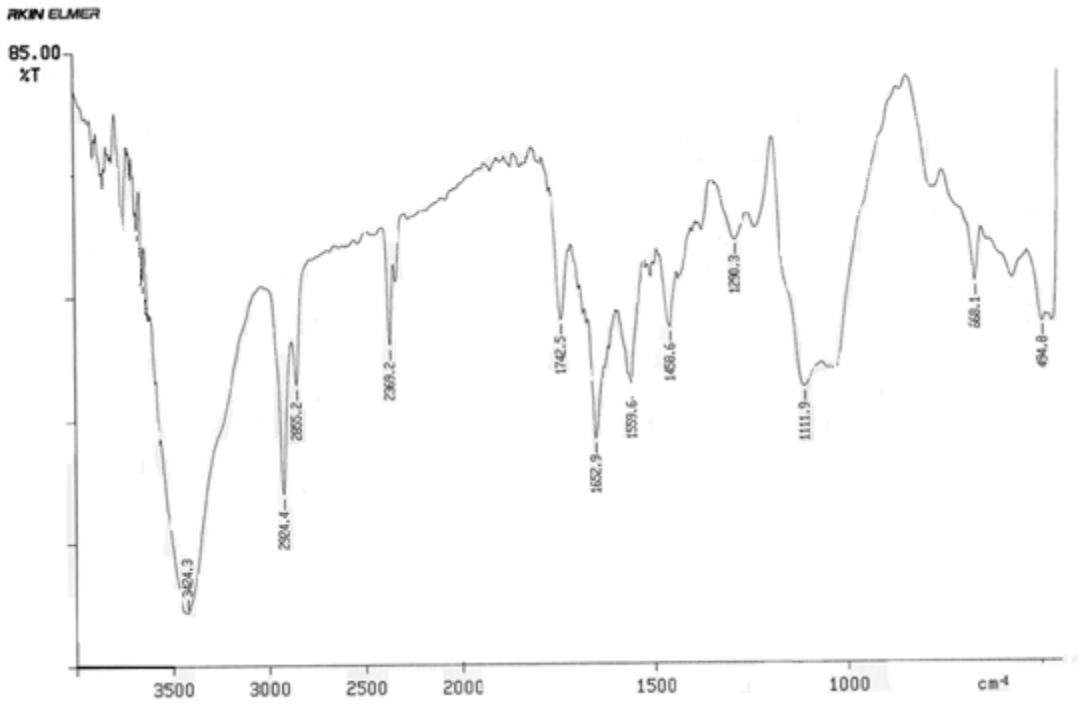

Fig 3.8: IR spectra of GOD-a-MWNT/PANI composite

The IR spectra of PANI/GOD-a-MWNTs shown above was recorded between the wavenumber rang of 500 to 4000cm^{-1}. In the IR spectra of PANI/GOD-a-MWNT composite the most important **peak at 1652.9 cm^{-1}** corresponds to the **amide-I band and the peak at 1559.6 cm^{-1}** corresponds to **the amide II band**.

These peaks confirm the synthesis of PANI/GOD-a-MWNTs composite.

3.2 Electrochemically Electrode Fabrication and Cyclic-Voltammetry

Electrochemical technique is very useful and easy technique for the fabrication of electrodes. Cyclic Voltammetry have been carried out for determining the redox potential of the PANI, PANI/MWNTs composite and PANI/GOD-a-MWNTs composite. The results of these studies are explained in the following sections.

3.2.1 Polymerization of aniline by Cyclic Voltammetry

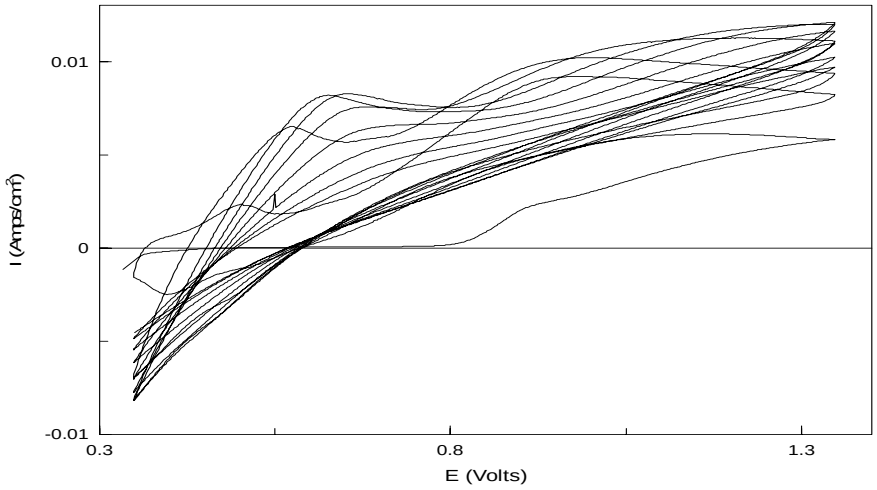

Fig 3.9: Growth curve of Polyaniline

The polymerization of aniline and its film deposition in 1M HCl on ITO coated electrode was recorded in the voltage range 0.4V to 1.4V for 10 cycles at scan rate of 10 mV/sec. The reduction or oxidation of a substance at the surface of a working electrode, at the appropriate applied potential, results in the mass transport of new material to the electrode surface and the generation of a current [30]. For irreversible systems the peak potential are characterized by a shift of the peak potential with the scan rate:

The peak potential:

$$E_p = E^\circ - (RT/\alpha n_a F)[0.78 - \ln(k^o/(D)^{1/2}) + \ln(\alpha n_a F\nu/RT)^{1/2}] \quad \textbf{(1)}$$

The peak current:

$$\mathbf{i}_p = (2.99x10^5)\mathbf{n}(\alpha n_a)^{1/2}ACD^{1/2}n^{1/2} \quad \textbf{(2)}$$

where α is the transfer coefficient, n_a is the number of electrons involved in the charge-transfer step, k^0 is the heterogeneous rate constant, R is the molar gas constant (8.3144 J $mol^{-1}K^{-1}$), n is the number of electrons, T is the absolute temperature (K), F = Faraday constant (96,485 C/equiv), and E^0 is the standard potential ,A is the electrode area (in cm^2), C is the concentration (in mol/cm^3), D is the diffusion coefficient (in cm^2/s), and v the scan rate (in V/s).

From above equations it is clear that peak potential will be higher than E^0 and the current is directly proportional to the concentration [31].

In the above graph the oxidation current was found to be increased gradually with cycles indicating the continuous growth of the polymer film on the electrode surface in each cycle. The thickness of the film is corresponding to the number of cycles used for film deposition [32].

.

3.2.2 Deposition of PANI (Potentiostatic mode)

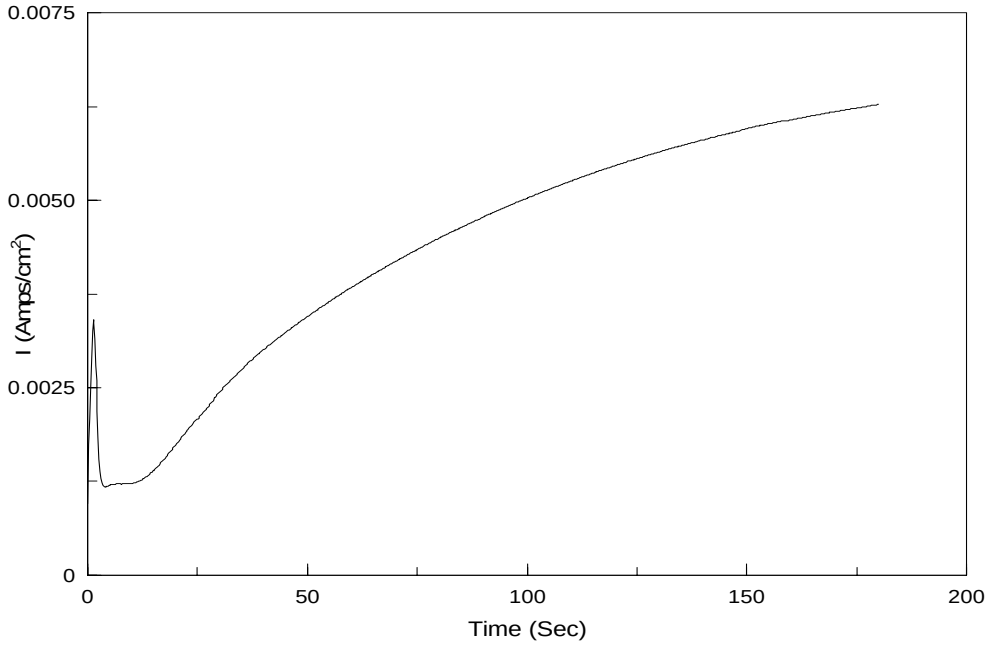

Fig 3.10: Growth curve of PANI

The growth curve of PANI was obtained at room temperature in PBS buffer (0.1M pH 6.8) using ITO coated glass electrode as working electrode and at constant potential of 2V for 3 min. The curve shows the continuous increase in current with time which indicates the polymerization of aniline and its film deposition on electrode.

3.2.3 Cyclic Voltammetry of PANI

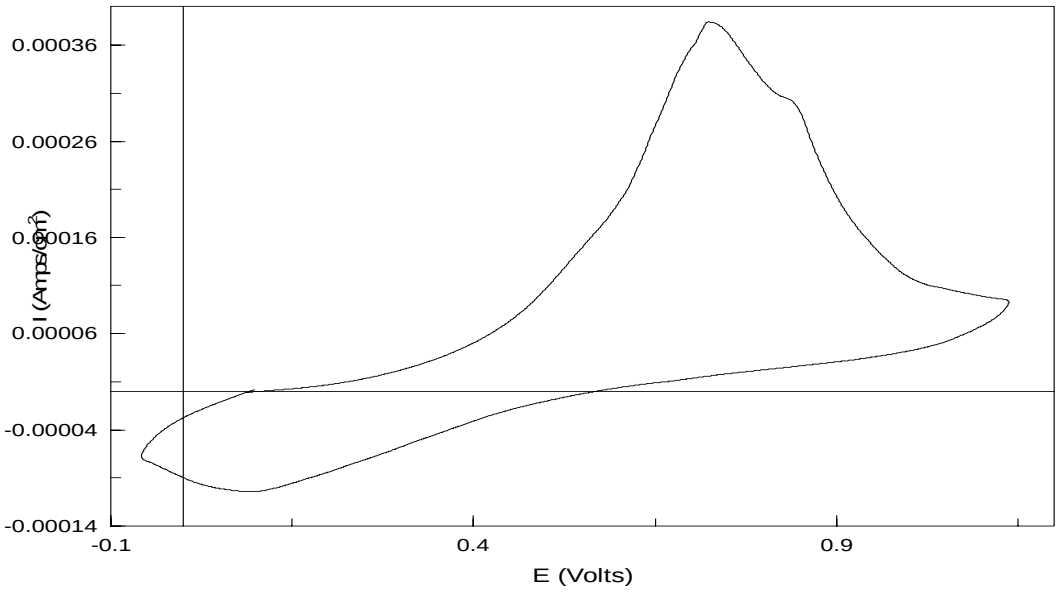

Fig 3.11: Cyclic Voltammogram of PANI in PBS Buffer

The cyclic voltamogramm of PANI was recorded at room temperature in the voltage range - 0.05V to 1.2V in PBS buffer (0.1M pH 6.8) at the scan rate of 10 mV/sec. The oxidation peak of polyaniline was observed at voltage 0.73161V. The peak related to the conjugation length of the polymer [32].

3.2.4 Deposition of PANI/a-MWNTs composite

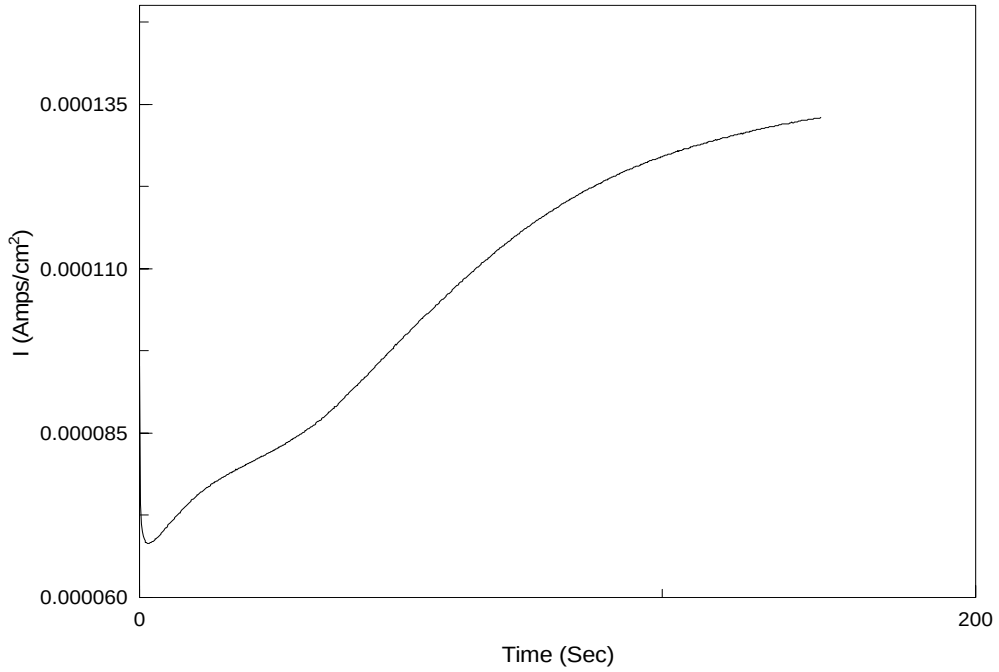

Fig 3.12: Growth curve of PANI/a-MWNTs Composite

The growth curve of PANI/a-MWNTs composite was obtained at room temperature in PBS buffer (0.1M pH 6.8) using ITO coated glass electrode as working electrode and at constant potential of 2V for 3 min. The curve shows the continuous increase in current with time which indicates the polymerization and film deposition of composite on electrode. The a-MWNTs are trapped in between the polymer chains while the formation of composite.

3.2.5 Cyclic Voltammetry of PANI/a-MWNTs composite

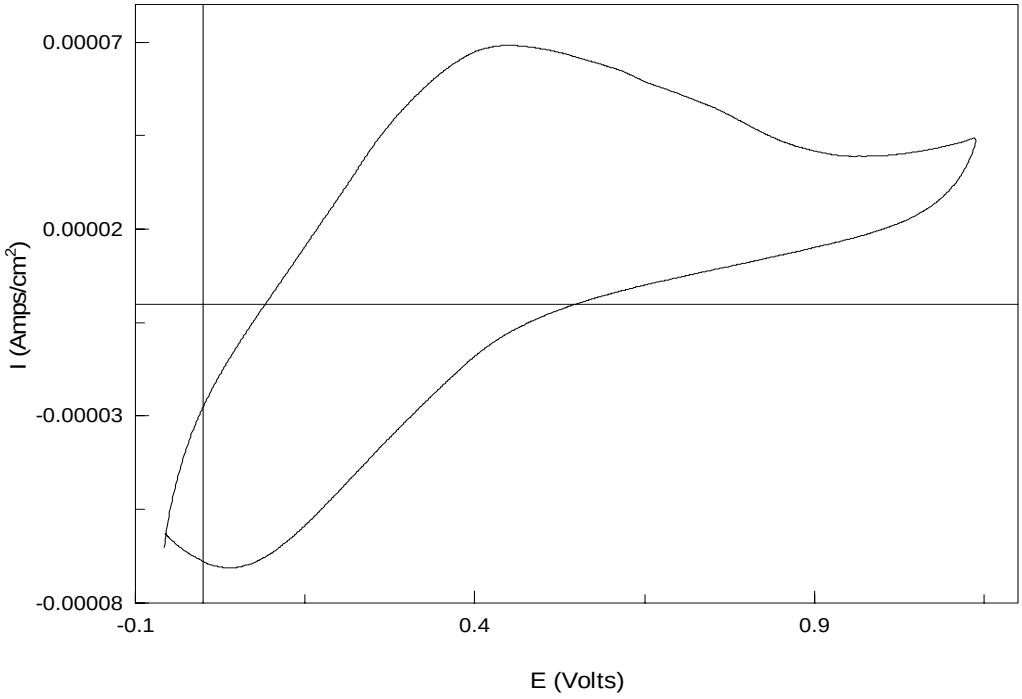

Fig 3.13: Cyclic Voltammogram of composite of PANI/ a-MWNTs

The cyclic voltamogramm of PANI/a-MWNTs composite was recorded at room temperature in voltage range - 0.5V to 1.2V in PBS buffer (0.1M pH 6.8) at the scan rate of 10 mV/sec. In the cyclic voltammogram of composite the oxidation peak is observed at the potential 0.48476V. On comparison, it was found that the oxidation peak obtained for composite is shifted towards the lower potential as compared to PANI (0.73161V). The shift of oxidation peak towards lower potential suggests that the conjugation length of composite is higher than the individual PANI. The increse in conjugation length results the higher value of electrical conductivity [32].

3.2.6 Deposition of PANI/GOD-a-MWNTs composite

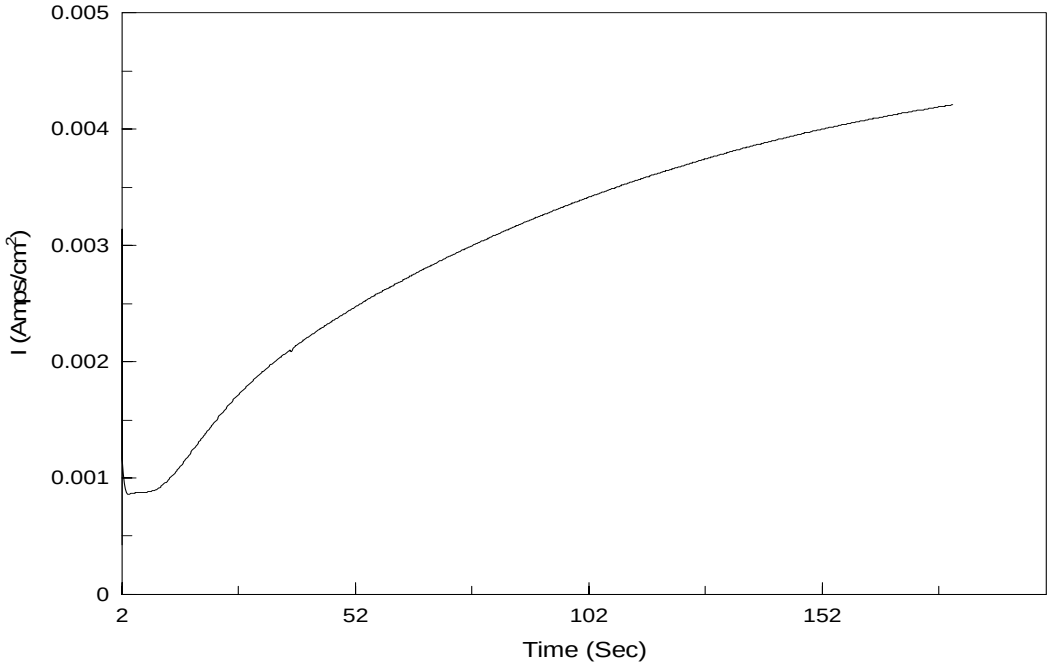

Fig 4.14(a): Growth curve of PANI/ GOD-a-MWNTs composite

The growth curve of PANI/GOD-a-MWNTs composite was obtained at room temperature using ITO coated glass electrode as working electrode at constant potential of 2V for 3 minutes in PBS buffer (0.1M pH 6.8). The curve shows the continuous change in current with time which indicates the polymerization and film deposition of composite on electrode. In composite the GOD-a-MWNTs are trapped in the polymer chains reducing the length of polymer chains.

3.2.7 Cyclic Voltammetry of PANI/GOD-a-MWNTs composite

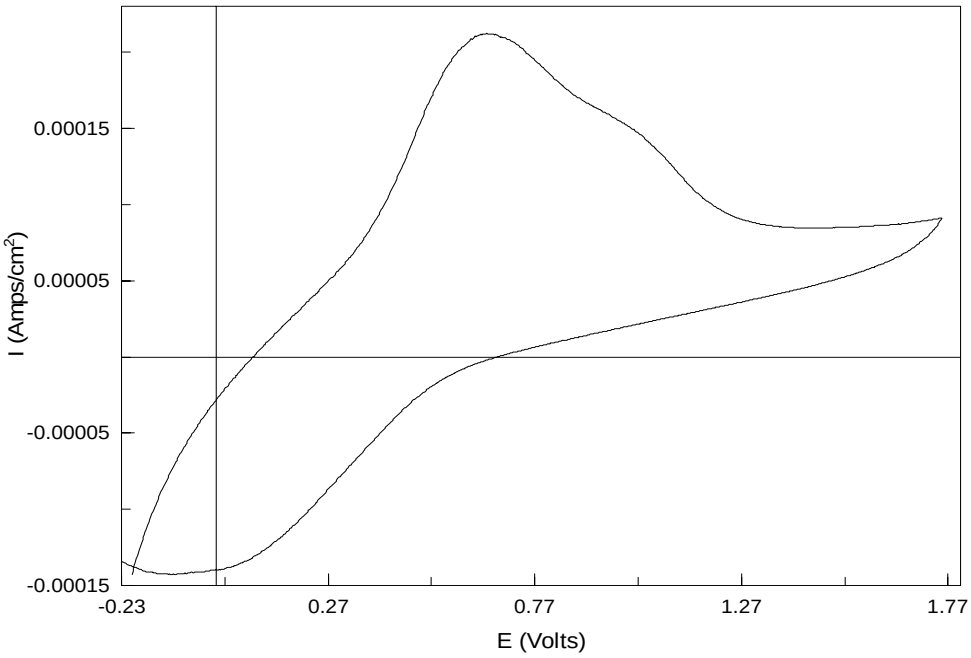

Fig 3.15: Cyclic Voltammogram of composite of PANI/GOD-a-MWNTs

The cyclic voltamogramm of composite of PANI and GOD- a-MWNTs was recorded in voltage range -0.2V to 1.6V in PBS buffer (0.1M pH 6.8) at the scan rate of 10 mV/sec. In this voltamogram only one oxydation peak is obtained at voltage 0.64321V. The oxidation peak corresponding to composite of PANI/GOD-a-MWNTs is found to shifted towards the lower potential as compared to PANI (0.73161V) and higher as compare to composite of PANI/a-MWNTs (0.48476V). The shift of oxidation peak towards higher potential suggests that the conjugation length of composite of PANI/GOD- a-MWNTs is higher than the individual PANI and lower than the composite of PANI/a-MWNTs . The decrease in conjugation length results the lower value of electrical conductivity of PANI/GOD- a-MWNTs composite as compare PANI/ a-MWNTs composite.

3.3 Morphological Studies

Surface morphological studies have been carried out for determining the surface texture of the MWNTs and GOD-a-MWNTs. The results of these studies are explained in the following section:

3.3.1 FE-SEM image of Pristine MWNTs and GOD-a- MWNTs

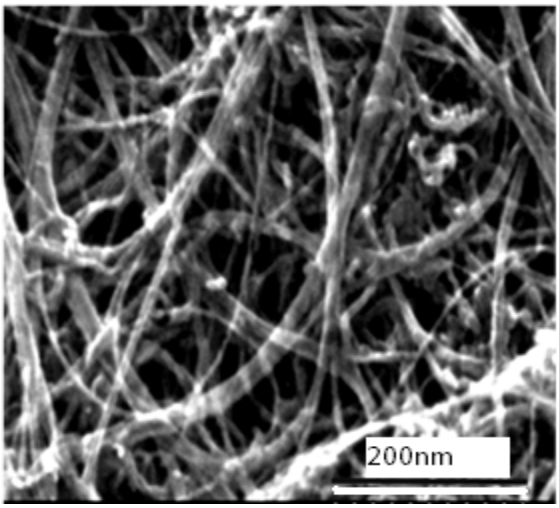

Fig 3.16: Pristine MWNTs

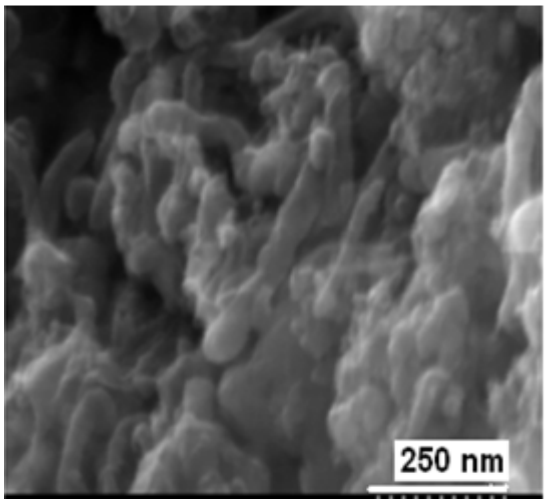

Fig 3.17: GOD-a-MWNTs

From the SEM micrographs shown above it can be seen that the acid treatment have changed the morphology of multi-walled carbon nanotubes as compared to the raw multi-walled carbon nanotubes. By the acid treatment, the length of the multi-walled carbon nanotubes was decreased and the less well defined structure of MWNTs was obtained. In fig 3.16 shows the attachment of glublar shaped GOD on MWNTs as compare to fig 3.17.

3.4 Enzymatic activity measurements

The measurement of activity of enzymes is important for fabrication of biosensor. The graphs shown below are between incubation time and absorbance. These graphs show the activity of enzyme. In the presence of POD, Die and D-glucose, chemical reaction takes place and the color of solution changes, this change increases the absorbance.

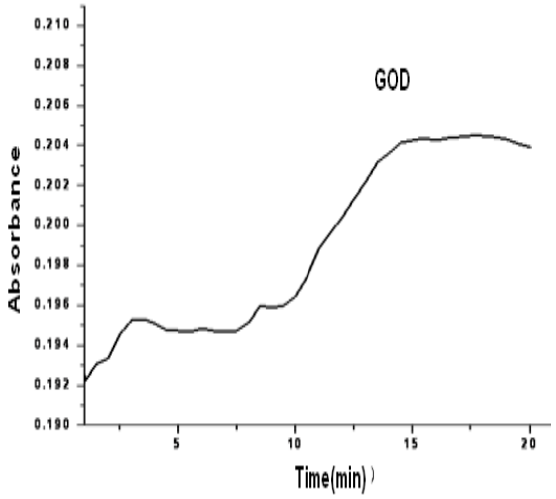

Fig 3.18: Activity curve of pure GOD

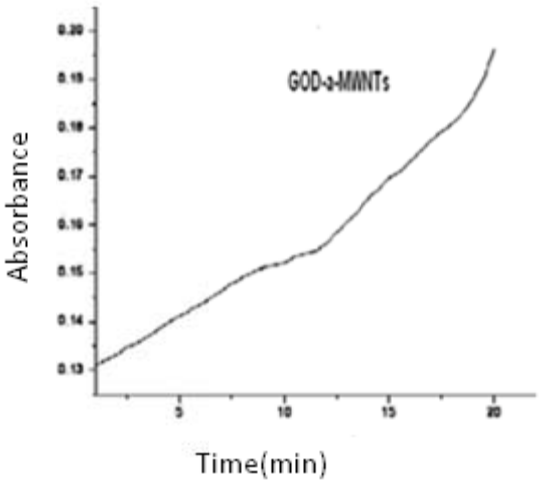

Fig 3.19: Activity curve of GOD-a-MWNTs

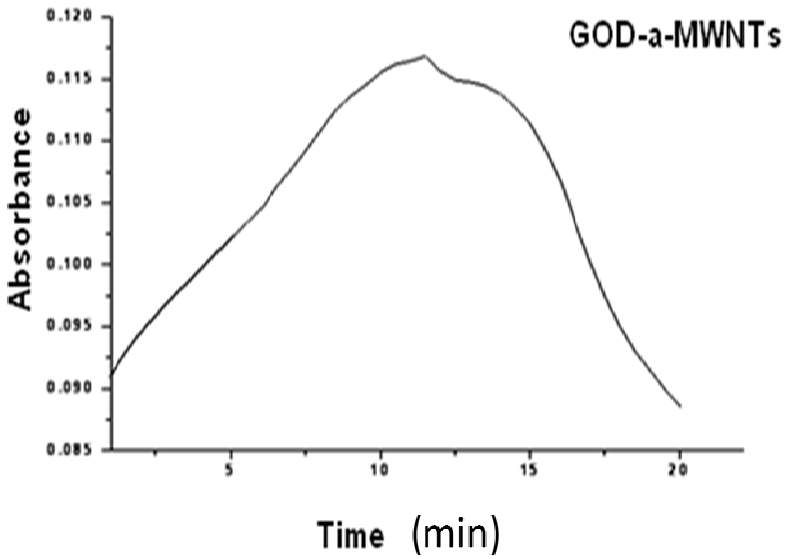

Fig 3.20: Activity curve of GOD-a-MWNTs after 8 weeks

The above curves show that the pure GOD and GOD-a-MWNTs both remained active up to 20 minutes. The activity measurement experiment was repeated up to 8 weeks in the same conditions and the GOD-a-MWNTs was found active but its activity time was found to be lowered after 8 weeks.

CHAPTER-4

CONCLUSIONS AND FUTURE SCOPE

4.1 Conclusions

The conclusions of the studies carried out in the course of this thesis are as follows:

1. MWNTs have good conducting properties; they can be used in charge transfer reaction. They can be used in electrochemical biosensor as an electrode which can detect the electron flow due to enzymatic reactions.
2. By functionalization, various biomolecules can be covalently linked to the carbon nanotubes.
3. The pristine MWNTs were successfully functionalizes through chemical route. Functionalization of MWNTs was confirmed by IR spectra.
4. The covalent attachment of glucose oxidase on a-MWNTs was successfully carried out. The attachment of GOD was confirmed by FT- IR and FE-SEM.
5. The activity of GOD-a-MWNTs was successfully measured by Continuous Spectrophotometric method. The activity of enzyme was confirmed by increase in absorption (A_{500}) with incubation time. Every week (maximum up to 8 weeks), the experiments related to the measurement of enzyme activity was repeated and GOD in GOD-a-MWNTs composite was again found active.
6. After the confirmation of activity of GOD-a-MWNTs material the work is directed towards the fabrication of enzyme electrode. The PANI was used for electrode fabrication because of its good electrical properties. The composite of PANI/GOD-a-MWNTs was prepared by electrochemical technique using ITO coated glass plate as working electrode. The fabrication of electrodes of PANI, PANI/a-MWNTs composite and PANI/GOD-a-MWNTs composite was confirmed by FT-IR and Cyclic Voltammetry.

7. The shift in oxidation peak voltage of PANI/GOD-a-MWNTs composite as compare to that of PANI and PANI/a-MWNTs composite show the successful synthesis of PANI/GOD-a-MWNTs composite.
8. The above results show that the PANI/GOD-a-MWNTs composite electrode fabricated by the route given in the present work can be successfully used for the estimation of glucose.

4.2 Future scope

The results of the studies presented in this thesis further suggest some area of scientific and technological interest. They are as follows:

1. The electrodes fabricated in this work can be used as working electrode in amperometric electrochemical biosensor.
2. Further work is needed to understand the biosensing ability of the composite formed and to quantify the response of electrode to various concentration of glucose.
3. The method of immobilization of enzyme presented in this work can be used for immobilization of other enzymes on MWNTs and fabrication of biosensor.
4. The CNTs modified polymer electrodes can be used for gas sensing devices rechargeable batteries and other electronic devices.

References

1. M. Olek "Carbon nanotubes composite – Mechanical, Electrical, and optical properties" 2006.
2. Shiren Wang **"**Functionalization of Carbon Nanotubes: Characterization, modeling and composite applications" The Florida State University College of Engineering, 2006.
3. A. R. Gustavo, M. D. Rubianes, C. R. Marcela , F. F Nancy, L. L. Guillermina, L. P. Mar, A. M. Silvia, C. Parrado "Carbon nanotubes for electrochemical biosensing" Talanta 74 (2007) 291.
4. J.H.Chen, H.P.Haung, D.Z.Wang, S.X.Yang, W.Z.Li, J.G.Wen and Z.F.Ren "Electrochemical synthesis of polypyrrole film over each well aligned carbon nanotubes" synthetic metals 125(2002)289.
5. Rongmei LIU "The Functionalization of Carbon Nanotubes" February, 2008.
6. D. B. Mawhinney, V. Naumenko , A. Kuznetsova , J. T. Yates , J. Liu , R.E. Smalley "Surface defect site density on single walled carbon nanotubes by titration " Chemical Physics Letters 324(2000)213.
7. Di Wei and Ari Ivaska "Electrochemical Biosensors Based on Polyaniline" Chem. Anal. (Warsaw), 51(2006)839.
8. W. Matthew, P.N. Simina, X.G. Shapter "Measurement of functionalised carbon nanotube carboxylic acid groups using a simple chemical process" Carbon 44 (2006) 1137.
9. M. Daenen "The Wondrous World of Carbon Nanotubes" a review of current carbon nanotube technologies, 27 February 2003.
10. Colin Pratt "Conducting Polymer" 22-2-96.
11. J.C.W. Chien, P.C. Uden and J.L. Fan., J. Polym. Sci. Polym. Chem. Edn. 20 (1982) 2159.
12. G. Tourillon and F. Garnier., J. Electrochem. Soc. 130 (1983) 2042.
13. H. Munstedt, H. Naarmann and G. Kohler., Mol. Cryst. Liq. Cryst. 118 (1985) 129.

14. N.C. Foulds and CR Lowe., J. Chem. Soc. Faraday Trans-1 82 (1986) 1259.
15. P.D. Gaikwad, D.J. Shirale, V.K. Gade, P.A. Savale, H.J. Kharat, K.P. Kakde, and M.D. Shirsat "Immobilization of GOD on Electrochemically Synthesized PANI Film by Cross-linking via Glutaraldehyde for Determination of Glucose" Int. J.Electrochem. Sci., 1(2006)425.
16. H. C. Kim and H. B. Gu "Electrochemical properties of Glucose Biosensors: Pollypyrrol/ Glucose oxidase membrane" 500(1999)757.
17. X.Luo, A.J.Killard, A.Morrin, M.R.Smyth "Enhancement of a conducting polymer-based biosensor using carbon nanotube-doped polyaniline", Analytica Chimica Acta 575 (2006) 39.
18. A.K.Nanjundan, H.K.Sung, G.C.Byung, T.L.Byung, T.J.Yeon "Surface functionalization of multiwalled carbon nanotubes with poly(3,4 propylenedioxythiophene) and preparation of its random copolymers: new hybrid materials" Colloid Polym Sci 287(2009) 97.
19. X. hong, L. B. Wu, J. Huang, J. Zhang, Z. Liu, H. Li "Fabrication and characterization of well-dispersed single-walled carbon nanotube/ polyaniline composites" Carbon 411 (2002) 1645 .
20. Saraju P. Mohanty "Biosensors: A Tutorial Review".
21. Miroslav Pohanka and Petr Skládal "Electrochemical biosensors – principles and applications" Appl. Biomed. 6(2008)57.
22. S.G. Wang, Q. Zhang, R. Wang, S.F. Yoon, J. Ahn, D.J. Yang, J.Z. Tian, J.Q. Li and Q. Zhou "Multi-walled carbon nanotubes for the immobilization of enzyme in glucose biosensors" Electrochemistry Communications 5 (2003) 800.
23. Y.P.Sun, K. Fu, Y. Lin, and W Huang "Functionalized Carbon Nanotubes: Properties and Applications" Acc. Chem. Res. 35(2002)1096.
24. Y. Wang, Z. Iqbal, S.V. Malhotra "Functionalization of carbon nanotubes with amines and enzymes" Chemical Physics Letters 402 (2005) 96.
25. J. Li, Y.B Wang, J.D. Qiu, D. Sun, X.H. Xia "Biocomposites of covalently linked glucose oxidase on carbon nanotubes for glucose biosensor" Anal Bioanal Chem 383(2005) 918.

26. K. Jiang, L. S. Schadler, R. W. Siegel, X. Zhang, H. Zhangc and M. Terrones, "Protein immobilization on carbon nanotubes via a two-step process of diimide-activated amidation" material chemistry, 2003.
27. Y. Lin, F. Lu, Y. Tu, and Z. Ren "Glucose Biosensors Based on Carbon Nanotube Nanoelectrode Ensembles" Nano Letters, 4 (2004)191.
28. J. Zhang, M.Feng and H.Tachikawa "Layer-by-layer fabrication and direct electrochemistry of Glucose oxidase on single wall carbon nanotubes" Biosensors and Bioelectronics 22 (2007) 3036.
29. P.D.Gaikwad, D.J.Shirale, P.A.Savale, K.Datta, P.Ghosh, A.J.Pathan, G.Rabbani and M.D.Shirsat "Development of PANI-PVS-GOD electrode by potentiometric method for determination of glucose" Int. J.Electrochem.Sci. 2(2007)488.
30. www.chemistry.nmsu.edu/studntres/chem435/Lab13/.
31. S.P. Kounaves "Voltammetric Techniques"Tufts UniversityDepartment of Chemistry.
32. Amit L. Sharma, Thin Solid Films, 517 (2009) 3350.

APPENDIX A

Materials used

- **Carbon nanotubes (CNTs) -** During these work multiwall carbon nanotubes (MWNTs) of length 0.5 to 2μm and average outer diameter 8 nm, were used. The purity level was 95%.
- **Glucose oxidase (GOD) -** glucose oxidase has been provided by US Biological. The biological source of it is fungus Aspegillus niger and Its type is X-5.
- **Filters** – The filters were used poly tetra floro-ethylene filter (PTFE) hydrophilic and hydrophobic membrane with pore size 0.22μm.

Chemicals used

- **Sulfuric acid (H_2SO_4) -** Purchased from Qualigens of product no. 29307, with purity 99%.
- **Nitric acid (HNO_3) -** Purchased from LOBA CHEMIE with product no. 7697- 37 -2, in liquid form with purity 69 – 72%.
- **Hydrochloric acid (HCl) -** Purchased from LOBA CHEMIE of product no.7647- 01- 0 in liquid form.
- **Acetone (CH_3COCH_3) –** Purchased from Merck of product no. A0160 in liquid firm of purity 99%.
- **Ethanol -** Purchased from Les Alcols De Commerse Ind in liquid firm of purity 99.9%.
- **Tetrahydrofuran (C_4H_8O) -** Purchased from Spectrochem in liquid form of purity 99.5%.
- **Peroxidase -** Purchased from Himedia in powder form.
- **Dimethylformamide ($HCON(CH_3)_2$) -** Purchased from LOBA CHEMIE purity 99.5%.
- **O-Dianisidine dihydrochloride dye -** Purchased from Sigma in powder.

- **Sodium Chloride (NaCl) -** Purchased from Himedia in powder form with 99.9% purity.
- **Sodium phosphate dibase heptahydrate ($Na_2HPO_4.7H_2O$) -** Purchased from LOBA CHEMIE in powder form of purity 99.5%.
- **Potassium Chloride (KCl) -** Purchased from LOBA CHEMIE in powder form with purity 98%.
- **Potassium dihydrogen orthophosphate -** Purchased from Himedia in powder form with 99.9% purity.
- **Sodium hydroxide pellets-** Purchased from LOBA CHEMIE.
- **Thionyl Chloride ($SOCl_2$) -** Sd fine chem. In liquid form.
- **Sodium Acetate (CH_3COONa) -** Purchased from LOBA CHEMIE.
- **Deionized water**
- **PBS Buffer solution (0.1M, pH 6.8)-** 400 mg NaCl, 10 mg KCl, 72 mg disodium hydrogen phosphate and 12 mg potassium dihydrogen phosphate was added in 500 water. It was stirred vigorously on a magnetic stirrer. Its pH was adjusted to 6.8 with few drops of 1M HCl or 1M NaOH solution. It was sterilized by autoclaving at 15 lbs/in^2 at 120^{0}C for 15 minutes on laboratory autoclave apparatus (METREX). The buffer was stored at 4^{0}C.
- (A) 50 mM Sodium Acetate Buffer, pH 5.1 at 35°C (Prepared 200 ml in deionized water using Sodium Acetate. Adjusted to pH 5.1 at 35°C with 1 M HCl).
- (B) 0.21 mM o-Dianisidine Solution (Dissolved the contents of one 50 mg vial of o-Dianisidine Dihydrochloride, in 7.6 ml of deionized water. Diluted 1.0 ml to 100 ml with Reagent A.)
- (C) 10% (w/v) ß-D(+)Glucose Substrate Solution (Prepare 10 ml in deionized water using ß-D(+)Glucose,
- (D) 0.17 mM o-Dianisidine and 1.72% (w/v) Glucose Solution(Reaction Cocktail) (Immediately before use, prepared 29 ml by combining 24.0 ml of Reagent B with 5.0 ml of Reagent C. Equilibrated to 35°C and adjusted to pH 5.1 if necessary with 1 M HCl or 1 M NaOH.

- (E) Peroxidase Enzyme Solution (POD) - (Immediately before use, prepare a solution containing 60 Purpurogallin units/ml of Peroxidase, in cold deionized water.)
- (F) Glucose Oxidase Enzyme Solution prepared an initial solution of 20 - 40 units/ml in cold Reagent A. Then immediately prior to use, further dilute to 0.4 - 0.8 unit in cold Reagent A.

❖ **Instrumentation**

- Fourier Transform infra- red (FT-IR) spectrometer: Perkin Elmer spectrum RXI FT-IR system.
- UV – Visible spectrometer: Perkin Elmer Lambda - 35
- Scanning electron microscopy (FE-SEM): HITACHI S/N 4300, field emission scanning electron microscope.
- Cyclic Voltammetry: Solatron, 1285 Potentiostate, using Corrview software.

❖ **Apparatus Used**

- **H**igh strength sonicator
- Hot air oven
- Microbalance
- Magnetic stirrer with hot plate
- Vacuum pump
- Autoclave
- Filtration setup
- Vacuum desiccator
- Appendroph
- Beaker
- Conical Flask
- Refluxing setup
- pH meter – deluxe (model 101E)

- ITO plates (1.5×1 cm^2)
- Petri disc
- Measuring cylinder
- Test tubes

APPENDIX -B

Characterization of a material is an important step because it gives useful parameters in determining the properties of material. During this research work various techniques such as FT-IR spectrometer, Cyclic-Voltammetry and FE-SEM etc were used. In this chapter, the description, principal and working of these techniques have been discussed.

These characterization techniques are discussed below in detail:

1. Fourier Transform Infrared (FT-IR) Spectroscopy

Infrared (IR) spectroscopy is a useful technique for characterizing materials and providing information on the molecular structure, dynamics, and environment of a compound. When irradiated with infrared light (photons), a sample can transmit, scatter, or absorb the incident radiation. Absorbed infrared radiation usually excites molecules into higher energy vibrational states. This can occur when the energy (frequency) of the light matches the energy difference between two vibrational states (or the frequency of the corresponding molecular vibration).

Infrared spectroscopy is particularly useful for determining functional groups present in a molecule. Many functional groups vibrate at nearly the same frequencies independent of their molecular environment. This makes infrared spectroscopy useful in materials characterization. Further, many subtle structural details can be gleaned from frequency shifts and intensity changes arising from the coupling of vibrations of different chemical bonds and functional groups.

Recent advances in computerized IR spectroscopy, particularly Fourier transform infrared (FT-IR) spectroscopy, have made it possible to obtain infrared spectra using various sampling techniques. Infrared spectra have traditionally been produced by transmission, that is, transmitting light through the sample, measuring the light intensity at the detector, and comparing it to the intensity obtained with no sample in

the beam, all as a function of the infrared wavelength. Techniques such as attenuated total reflectance, diffuse reflectance, specular reflectance, reflection-absorption, and photo acoustic spectroscopy have recently become more common. This article will discuss the sampling techniques, applications, and the molecular structure information the resulting infrared spectra can provide.

Basic Principles

Infrared spectra are typically presented as plots of intensity versus energy (in ergs), frequency (in s^{-1}), wavelength (in microns), or wave number (in cm^{-1}). Wave number units are preferred, but several books of reference spectra are plotted in wavelength. Units can be converted easily using:

$$\boldsymbol{E = \nu h = \frac{hc}{\lambda}} \quad \textbf{(1)}$$

where E is energy in ergs, h is Planck's constant (6.63×10^{-27} erg · s), ν is the frequency in s^{-1}, λ is the wavelength in centimeters, and c is the velocity (speed) of light (3×10^{10} cm/s); and:

$$\boldsymbol{\bar{\nu} = \frac{1}{\lambda}} \quad \textbf{(2)}$$

Where $\boldsymbol{\bar{\nu}}$ is the wavenumber in cm^{-1}. When λ is expressed in microns (the unit normally used for wavelength), Eq 2 becomes:

$$\boldsymbol{\bar{\nu} = \frac{10000}{\lambda}} \quad \textbf{(3)}$$

In practice, wavenumber is often called frequency, and the symbol ν used instead of $\boldsymbol{\bar{\nu}}$. Although, formally, the infrared region of the electromagnetic spectrum is between the wavelengths of 0.78 and 1000 μm (12,820 to 10 cm^{-1}), this article will consider the mid-infrared region from 2.5 to 25 μm (4000 to 400 cm^{-1}). This region, where most fundamental vibrational modes occur, is the most useful for materials characterization.

Intensity can be expressed as percent transmittance (%T) or absorbance (A). If I_0 is the energy, or radiant power, reaching the infrared detector with no sample in the beam, and I is the energy detected with a sample present, transmittance is:

$$\mathbf{T}= \frac{I}{Io} \quad \textbf{(4)}$$

and percent transmittance

$$\mathbf{\%T}= \frac{100I}{Io} \quad \textbf{(5)}$$

Absorbance is:

$$A = \log\left(\frac{1}{T}\right) = \log\left(\frac{I_0}{I}\right)$$

Strong and weak bands are more easily visualized simultaneously without changing scale when spectra are plotted in transmittance, because the absorbance scale ranges from zero to infinity, while transmittance ranges from 0 to 100% T (0%T corresponds to an absorbance of infinity). For quantitative analyses (including spectral subtraction), absorbance or some other intensity scale proportional to concentration must be used.

The molecular geometry, atomic masses, and a complete description of the forces between the atoms (force field) are required to calculate the vibrational frequencies and describe the fundamental vibrations of a molecule. This is normal coordinate analysis. In practice, the molecular structure is usually not known, and the infrared spectra are used to assist in determining it. However, accomplishing this requires an understanding of how molecular vibrations contribute to the observed infrared spectrum. Molecular vibrations are complicated, because individual bond stretches or bond-angle bends are often highly coupled to each other. Progress in understanding the nature of molecular vibrations has derived mainly from empirical observation. Although of little practical use in materials characterization, normal-coordinate analysis reveals the nature of molecular vibrations, which can be useful in analyzing complicated infrared spectra.

Instrumentation

Obtaining an infrared spectrum necessitates detection of intensity changes as a function of wavenumber. Commercial infrared instruments separate light into single

infrared wavenumber intervals using a dispersive spectrometer (prism, grating, or variable filter), a Fourier transform spectrometer, or a tunable infrared laser source.

In dispersive infrared spectroscopy, a mono chromator separates light from a broad-band source into individual wave number intervals. The mono chromator contains a dispersing element, such as a prism, diffraction grating, or variable filter, which rotates to enable a mechanical slit to select individual wave number regions sequentially. The spatial distance separating the individual wavelengths after dispersion and the mechanical slit width determine spectral resolution and optical throughput. For a given instrument, the higher the spectral resolution, the lower the signal-to-noise ratio of the spectrum.

Fourier transform infrared spectroscopy uses an interferometer to modulate the intensity of each wavelength of light at a different audio frequency. A beam splitter divides the light from a broad-band infrared source into two optical paths. Recombination of the beams at the beam splitter generates a modulated optical path difference. The recombined beam undergoes constructive and destructive interference as a function of the instantaneous optical path difference. Several methods can be used to generate the modulated optical path difference. The most common is the Michelson interferometer as shown in Fig 1.1.

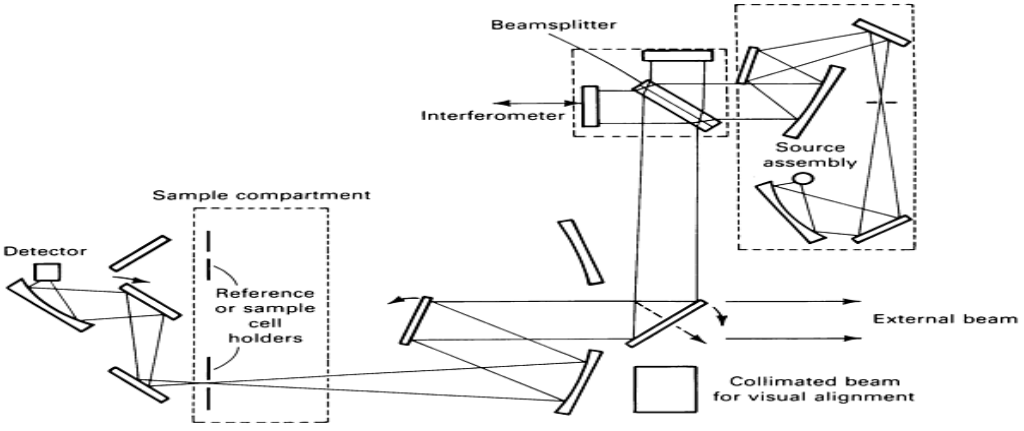

Fig 1.1: Optical diagram of a FT-IR spectrometer. Courtesy of Digilab

After being split into two optical paths by the beam splitter, the light from each path strikes two flat mirrors, one fixed and one moving, that return it to the beam splitter.

When the moving mirror is positioned so that the two optical paths are equal (zero path-difference position), all wavelengths of light simultaneously undergo constructive interference. At any other position of the moving mirror, a given wavelength of light may interfere constructively or destructively, depending on the phase relationship between the light rays in the two paths. For example, if the optical path difference is an integral multiple of the wavelength, constructive interference will result.

Spectrometer resolution equals the reciprocal of the distance the moving mirror travels. The modulation frequency for a particular wave number depends on mirror velocity. Modulation frequencies are typically from 50 Hz to 10 kHz. The detector signal, which is digitally sampled in fixed increments defined by interference fringes from a helium-neon laser, displays signal intensity as a function of moving mirror position. This signal is the interferogram. It must be Fourier transformed by a computer into the single-beam infrared spectrum.

Fourier transform infrared spectroscopy affords several advantages over dispersive IR spectroscopy. Information on the entire infrared spectrum is contained in an interferogram, which requires 1 s or less to collect. A spectrum with N resolution elements can be collected in the same amount of time as a single resolution element. This advantage is the multiplex, or Felgett's, advantage. Because the signal-to-noise ratio is proportional to the square root of the number of scans, the FT-IR time advantage can become a signal-to-noise ratio advantage of $N1/2$ for the same data collection time as with a dispersive spectrometer. The greater the total number of resolution elements in the spectrum, the more important becomes Felgett's advantage. Because no slit is required, FT-IR spectrometers have a light throughput advantage over dispersive spectrometers (Jacquinot's advantage). The helium-neon laser that controls sampling of the interferogram also provides precise calibration for the wavenumber position (Connes's advantage). Finally, because a digital computer is used to perform Fourier transforms, it is available for data processing. A computerized dispersive spectrometer can also handle data processing.

Interferometers other than the Michelson design are also available. The Genzel interferometer is similar, except the light beam is focused at the beam splitter, and the moving mirror modulates the optical path length in both arms of the interferometer. In other interferometers, optical path length is changed by moving a refractive element in one of the arms of the interferometer.

2. Field Emission Scanning Electron Microscopy (FE-SEM)

FE-SEM is used to visualize very small topographic details on the surface or entire or fractioned objects. Researchers in biology, chemistry and physics apply this technique to observe structures that may be as small as 1 nanometer (= billion of a millimeter). The FESEM may be employed for example to study organelles and DNA material in cells, synthetically polymers, and coatings on microchips

Fig 2.1: FE-SEM [S4300 Hitachi]

.

Electrons are liberated from a field emission source and accelerated in a high electrical field gradient. Within the high vacuum column these so-called primary electrons are focused and deflected by electronic lenses to produce a narrow scan beam that bombards the object. As a result secondary electrons are emitted from each spot on the object. The angle and velocity of these secondary electrons relates to the surface structure of the object. A detector catches the secondary electrons and

produces an electronic signal. This signal is amplified and transformed to a video scan-image that can be seen on a monitor or to a digital image that can be saved and processed further. The addition of energy dispersive X-ray detector combined with digital image processing is a powerful tool in the study of materials, allowing good chemical analysis of the material. The FE-SEM is a major tool in materials science research and development.

3. Electrochemical Techniques

The common characteristic of all voltammetric techniques is that they involve the application of a potential (E) to an electrode and the monitoring of the resulting current (i) flowing through the electrochemical cell. In many cases the applied potential is varied or the current is monitored over a period of time (t). Thus, all voltammetric techniques can be described as some function of E, *i*, and *t*. They are considered active techniques (as opposed to passive techniques such as potentiometry) because the applied potential forces a change in the concentration of an electroactive species at the electrode surface by electrochemically reducing or oxidizing it.

The analytical advantages of the various voltammetric techniques include excellent sensitivity with a very large useful linear concentration range for both inorganic and organic species (10^{-12} to 10^{-1} M), a large number of useful solvents and electrolytes, a wide range of temperatures, rapid analysis times (seconds), simultaneous determination of several analytes, the ability to determine kinetic and mechanistic parameters, a well-developed theory and thus the ability to reasonably estimate the values of unknown parameters, and the ease with which different potential waveforms can be generated and small currents measured.

Analytical chemists routinely use voltammetric techniques for the quantitative determination of a variety of dissolved inorganic and organic substances. Inorganic, physical, and biological chemists widely use voltammetric techniques for a variety of

purposes, including fundamental studies of oxidation and reduction processes in various media, adsorption processes on surfaces, electron transfer and reaction mechanisms, kinetics of electron transfer processes, and transport, speciation, and thermodynamic properties of solvated species.

3.1 Working

The electrochemical cell, where the voltammetric experiment is carried out, consists of a working (indicator) electrode, a reference electrode, and usually a counter (auxiliary) electrode. In general, an electrode provides the interface across which a charge can be transferred or its effects felt. Because the working electrode is where the reaction or transfer of interest is taking place, whenever we refer to the electrode, we always mean the working electrode. The reduction or oxidation of a substance at the surface of a working electrode, at the appropriate applied potential, results in the mass transport of new material to the electrode surface and the generation of a current. Even though the various types of voltammetric techniques may appear to be very different at first glance, their fundamental principles and applications derive from the same electrochemical theory.

3.2 Instrumentation

The basic components of a modern electro analytical system for Voltammetry are a potentiostat, computer, and the electrochemical cell. In some cases the potentiostat and computer are bundled into one package, whereas in other systems the computer and the A/D and D/A converters and microcontroller are separate, and the potentiostat can operate independently.

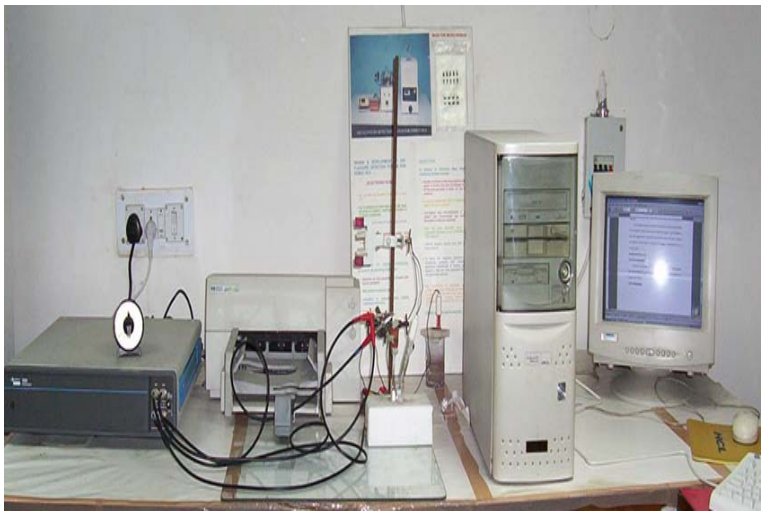

Fig 3.1: Electrochemical Interface (SOLARTRON Potentiostat 1285)

3.3 The Potentiostat

The task of applying a known potential and monitoring the current falls to the potentiostat. The most widely used potentiostats today are assembled from discrete integrated-circuit operational amplifiers and other digital modules. In many cases, especially in the larger instruments, the potentiostat package also includes electrometer circuits, A/D and D/A converters, and dedicated microprocessors with memory.

3.4The Electrodes and Cell

A typical electrochemical cell consists of the sample dissolved in a solvent, an ionic electrolyte, and three (or sometimes two) electrodes. The reference electrode should be as close as possible to the working electrode; in some cases, to avoid contamination, it may be necessary to place the reference electrode in a separate compartment. Reference Electrodes The **reference electrode** should provide a reversible half-reaction with Nernstian behavior, be constant over time, and be easy to assemble and maintain. The most commonly used reference electrodes for aqueous

solutions are the standard calomel electrode, and the silver/silver chloride electrode (Ag/AgCl). The **counter electrode** consists of a thin Pt wire, although Au and sometimes graphite have also been used.

Working Electrodes The working electrodes are of various geometries and materials, ranging from small Hg drops to flat Pt disks. Mercury is useful because it displays a wide negative potential range (because it is difficult to reduce hydrogen ion or water at the mercury surface), its surface is readily regenerated by producing a new drop or film, and many metal ions can be reversibly reduced into it. Other commonly used electrode materials are gold, platinum, and glassy carbon.

3.5 Cyclic Voltammetry

Cyclic Voltammetry (CV) has become an important and widely used electro analytical technique in many areas of chemistry. It is rarely used for quantitative determinations, but it is widely used for the study of redox processes, for understanding reaction intermediates, and for obtaining stability of reaction products.
This technique is based on varying the applied potential at a working electrode in both forward and reverse directions (at some scan rate) while monitoring the current. For example, the initial scan could be in the negative direction to the switching potential. At that point the scan would be reversed and run in the positive direction. Depending on the analysis, one full cycle, a partial cycle, or a series of cycles can be performed.

The important parameters in a cyclic voltammogram are the peak potentials (E_{pc} , E_{pa}) and peak currents (i_{pc} , i_{pa}) of the cathodic and anodic peaks, respectively. If the electron transfer process is fast compared with other processes (such as diffusion), the reaction is said to be electrochemically reversible, and the peak separation is

$$\Delta E_p = E_{pa} - E_{pc} = 2.303\ RT / nF \qquad [4]$$

Thus, for a reversible redox reaction at 25 °C with *n* electrons ΔE_p should be 0.0592/n V or about 60 mV for one electron. In practice this value is difficult to attain because

of such factors as cell resistance. Irreversibility due to a slow electron transfer rate results in $\Delta E_p > 0.0592/n$ V, greater, say, than 70 mV for a one-electron reaction.

The formal reduction potential (E_o) for a reversible couple is given by

$$E_0 = \frac{E_{pc} + E_{pa}}{2} \qquad [5]$$

For a reversible reaction, the concentration is related to peak current by the Randles–Sevcik expression (at 25 °C):

$$i_p = 2.686 \times 10^5 \; n^{3/2} \; A_c^0 \; D^{1/2} \; v^{1/2} \qquad [6]$$

Where i_p is the peak current in amps, A is the electrode area (cm^2), D is the diffusion coefficient ($cm^2\ s^{-1}$), c_0 is the concentration in mol cm^{-3}, and n is the scan rate in Vs^{-1}.

Cyclic Voltammetry is carried out in quiescent solution to ensure diffusion control. A three-electrode arrangement is used. Mercury film electrodes are used because of their good negative potential range. Other working electrodes include glassy carbon, platinum, gold, graphite, and carbon paste.

Electrochemical techniques are used for quantitative determination of organic and inorganic compounds in aqueous and nonaqueous solutions, measurement of kinetic rates and constants, determination adsorption processes on surfaces, determination electron transfer and reaction mechanisms, determination of thermodynamic properties of solvated species and fundamental studies of oxidation and reduction processes in various media. In the present work the electrochemical techniques were used for the film deposition and determination of redox potentials. For the use of this technique species of interest must be dissolved in an appropriate liquid solvent and capable of being reduced or oxidized within the potential range of the technique and electrode material [35].

4 UV/Visible Spectroscopy

UV/Visible spectroscopy is used for the quantitative analysis, qualitative analysis, fundamental studies of the electronic structure of atomic and molecular species and identification of the functional groups in organic molecules.

4.1 Basic Principle

Ultraviolet/visible absorption spectroscopy is almost exclusively the spectroscopy of molecules dissolved in solvents (most atoms in the gas phase also absorb in this spectral region; however, this is the province of atomic absorption spectroscopy.The spectral region of interest extends from 200 to 800 nm. The short-wavelength (200 nm) high-energy end of this spectral region is defined by the fact that below 200 nm oxygen and nitrogen in the atmosphere begin to absorb the radiant energy. The region below approximately 185 nm is termed the vacuum ultraviolet; the optical paths for experiments in the vacuum ultraviolet are evacuated or purged with a non absorbing gas, such as helium. The long wavelength low-energy end of the spectral region is defined by the fact that the eye can no longer detect light at wavelengths longer than the red end of the visible spectrum, near 700 nm.

The quantitative relationship between the energy of a photon of light and its wavelength is

$$\boldsymbol{E = \frac{hc}{\lambda}} \qquad \textbf{(1)}$$

Where h is 6.63×10^{-34} J · s (Planck's constant), c is 3.00×10^{17} nm/s (speed of light), and λ is the wavelength of the photon in manometers.

For a molecule to absorb energy of a specific wavelength, the molecule must have two energy levels separated exactly by the energy equal to the energy of the photon that will be absorbed; one of these energy levels must be occupied by an electron, and the second energy level must have a vacancy that can accept the electron (**Fig 4.1a). U**pon absorption of the photon (**Fig 4.1b),** the electron makes the transition (jumps) from the lower energy level to the upper. Although the outcome of the excited molecule **(Fig 4.1c**) will not be detailed in this article, the electron eventually must return to the lower energy level. A common result of this return to the ground state is the emission of a photon, again of precisely the same energy as the difference in energy between the two states (energy is always conserved). This phenomenon gives rise to other spectroscopic techniques, including molecular fluorescence.

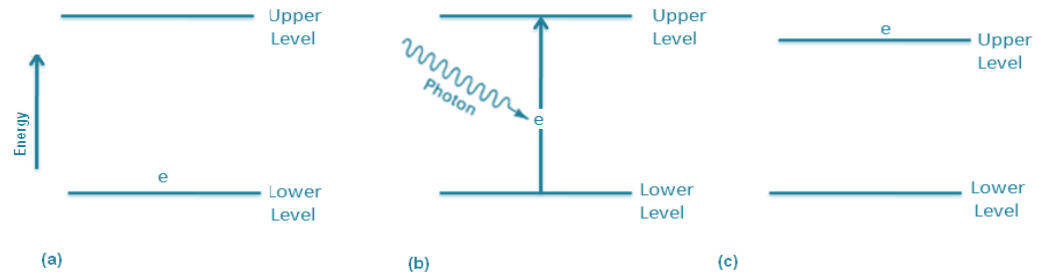

Fig 4.1: Absorption of a photon. (a) Ground state. (b) Transition. (c) Excited state

Certain symmetry conditions must also be satisfied before a molecule can absorb energy of a specific wavelength. If these conditions are not met, the probability of absorption of the photon by the molecule may be small, and it would be difficult or impossible to observe the spectroscopic transition experimentally.

Beer's law is the quantitative relationship that describes the quantity of light absorbed by a sample. Suppose, for example, that a sample of thickness b (Fig 4.2 a) is placed in a light path and that this sample absorbs half of the light incident on it. If a second sample identical to the first is then placed in the path of the light that passed through the first sample (Fig 4.2 b), the second sample will absorb half of the light incident on it, and the number of photons passing through both samples will be one-fourth the number of photons incident on the first sample.

This process could be continued indefinitely; each time another sample is added, the radiant power will be reduced by a factor of two. The radiant power is the rate of transfer of radiant energy and is therefore proportional to the number of photons passing through a unit area per second. Plotting the radiant power of the light that is transmitted as a function of the number of samples placed in the light path yields an exponential decay curve (Fig 4.3).

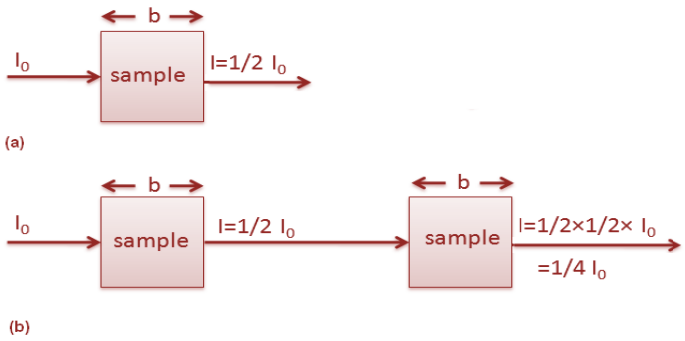

Fig 4.2: Absorption of light by samples of thickness *b*. (a) Sample placed in a light path that absorbs half of the incident light. (b) A second sample (identical to the first) in the light path that passed through the first samples.

This exponential decrease in radiant power can be expressed as:

$$P/P_0 = e^{-kb} \qquad \textbf{(2)}$$

Where P is the radiant power transmitted (not absorbed) by a sample of thickness b, P_0 is the radiant power incident on the sample, and *k* is a constant.

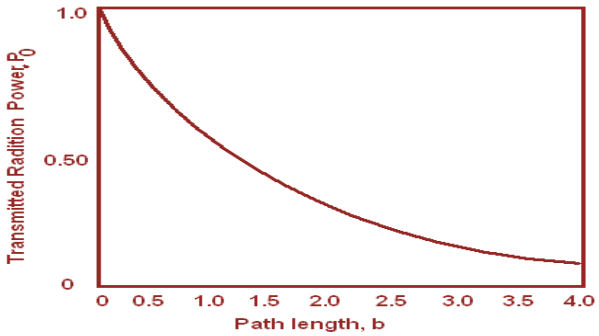

Fig 4.3: Exponential decay of radiant power as a function of path length

Note that the exponential decrease of the intensity is exactly like the exponential decay of a radioactive sample. After one half-life, half of the radioactive sample remains; after the second half-life, one quarter remains, and so forth. The mathematical equation for this decay has the same form as Eq 2:

$$N/N_0 = e^{-kt} \qquad \textbf{(3)}$$

Where N is the number of radioactive atoms remaining after time t, N_0 is the initial number of radioactive atoms, and k is a constant (related to the inverse of the half-life).

To this point, only one experimental variable (the thickness of the sample) has been discussed. The concentration of molecules in the sample will be examined next. As

before, it is assumed initially that the sample absorbs half of the radiant energy incident upon it and that the number of molecules through which the light must pass is doubled. In this instance, however, the number of molecules is increased by doubling the concentration of the sample instead of doubling the path length through which the light must pass. Nevertheless, the result is the same: each time the concentration is increased by one unit, the amount of light passing through the sample is decreased by a factor of two. **Figure 4.4** illustrates this exponential decrease in the radiant power.

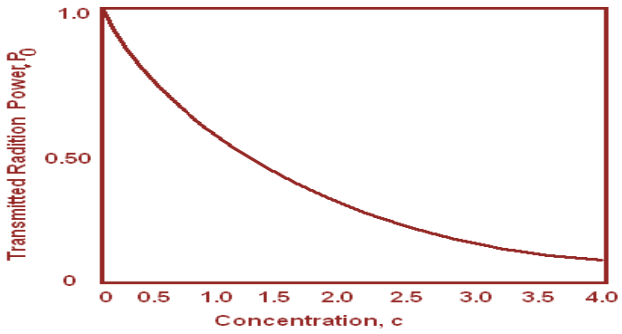

Fig 4.4: Exponential decay of radiant power as a function of concentration.

Thus, there are two important experimental variables, and the radiant power transmitted by the sample depends exponentially on each of them. This can be expressed mathematically by modifying Eq. (2) to include the concentration, c, of the sample:

$$P/P_0 = e^{-2.303abc} \qquad \textbf{(4)}$$

Where P is the radiant power transmitted (not absorbed) by a sample of thickness b and concentration *c*, P_0 is the radiant of power incident on the sample, and 2.303*a* is a constant. The ratio P/P_0 is the fraction of incident radiation transmitted by the sample and is set equal to T, the transmittance of the sample. Many spectrophotometers are designed to read %T (= 100 × T) directly.

Inverting Eq 4 and then taking the logarithm of both sides yields the following transformations:

$$P/P_0 = 1/T = e^{+2.303abc} \qquad \textbf{(5)}$$

$$\text{Log}_{10}(P_0/P) = \log_{10}(1/T) = abc \qquad \textbf{(6)}$$

Finally, the absorbance, *A*, is defined as follows: $A = \log_{10}(1/T)$. This yields the final form of Beer's law: $A = abc$ (7)

Where, *A* is the absorbance, *a* is the absorptivity (liters per gram centimeter), *b* is the optical path length through the sample (centimeters), and c is the sample concentration (grams per liter). The absorbance, an experimentally measurable quantity, is a linear function of the path length, b, and of the concentration, c, of the sample. Thus, if for a fixed path length the absorbance of several solutions were measured as a function of concentration, a linear calibration curve similar to that shown in Fig 4.5 would result. To determine the concentration of an unknown solution, it is necessary only to measure the absorbance of the solution, then read the concentration directly from the calibration curve.

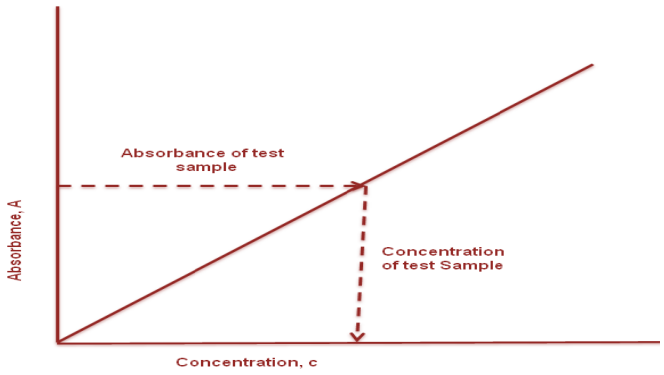

Fig 4.5: Calibration curve showing absorbance as a function of sample concentration.

The absorptivity, *a*, is the proportionality constant in Eq 7. Its units are selected so that the absorbance, A, is a unit less quantity. The absorptivity depends on the nature of the molecule, the wavelength at which the measurement is made, and, to a lesser degree, the solvent in which the molecule is dissolved.

Especially for the spectroscopy of organic molecules, Beer's law is often expressed as:

$$A = \varepsilon\, bc \qquad \textbf{(8)}$$

Where A is the absorbance, ε is the molar absorptivity (liters per mole centimeter), b is the optical path length through the sample (centimeters), and c is the sample concentration (moles per liter).